MONITORING AND EVALUATING MARINE DEBRIS IN A FINE-SCALE CONVERGENCE PHENOMENON AROUND MAKAI PIER, WINDWARD O'AHU

Brittney Lockett

A Thesis submitted in partial satisfaction of the requirements for the degree Master of Science in

Marine Science

College of Natural and Computational Sciences

Hawai‘i Pacific University

Fall 2023

Honolulu, Hawai'i

Advisory Committee:

David Field, Chair
David Hyrenbach
Sarah-Jeanne Royer

The views presented here are those of the author and are not to be construed as official or

reflecting the views of Hawai‘i Pacific University

ABSTRACT

Marine debris accumulation in large-scale convergence zones such as the Great Pacific Garbage Patch, and in submesoscale convergence features such as internal waves and estuarine fronts is well-documented, however, concentrated features on the finescale are just beginning to be studied. This study quantifies densities of microplastic (0.5 - 5 mm) and organic debris accumulation in a nearshore, finescale phenomenon around Makai Pier on four different days with different environmental conditions: light wind, average wind, above average wind, and above average north swell. Additionally, semi-quantitative patterns of marine debris were documented via weekly surveys by assigning ordinal values to various debris types and in different areas around the pier, resulting in a two-year time series of observations. Microplastic and organic debris were quantified within features (areas exhibiting concentrated debris), the swash zone along the shore, and in areas away from concentrated features (the background) around the pier by conducting manta net tows and collecting sieve samples through the surface of the water, and these estimates were used to calibrate the semi-quantitative data from the time series. To effectively compare the strength of converging mechanisms that this phenomenon demonstrates, we use the concentration factor as a dimensionless measurement, representing the ratio of the density of debris inside a convergence feature to the concentration of debris in the background. Microplastic densities within concentrated features reached ≥ 1000 #/m² on twenty-five percent of targeted survey days, with over fifty percent of the targeted days reaching densities ≥ 100 #/m². The concentration factor of debris within features was estimated to range from 1 to 10^6, with wave height being the most significant environmental predictor. Microplastic densities in the swash zone were consistently greater than in the background, yielding concentration factors between 1 and 100. These results are some of the first to quantify highly

concentrated debris within features on the order of meters, and the observed microplastic densities are, to the best of our knowledge, the highest densities in surface waters recorded in the literature making Makai Pier an excellent candidate for efficient marine debris removal.

Monitoring and Evaluating Marine Debris in a Fine-scale Convergence Phenomenon Around Makai Pier, Windward O'ahu

By

Brittney Lockett

12/7/2023

This thesis is submitted in partial fulfillment of the requirements for the degree of Master of Science in Marine Science at Hawai'i Pacific University. We the undersigned have examined this document and have found that it is complete and satisfactory in all respects, and all revisions required by the final examining committee have been made.

Author _____
Brittney Lockett

Committee Chair _____
David Field, PhD, Associate Professor of Marine Sciences, College of Natural and Computational Sciences

Committee Member _____
Karl David Hyrenback, PhD, Professor of Oceanography, College of Natural and Computational Sciences

Committee Member _____
Sarah-Jeanne Royer, PhD, Affiliate Faculty, Center for Marine Debris Research

Dean _____
Brenda Jensen, PhD, Dean, College of Natural and Computational Sciences

COPYRIGHT DECLARATION

This thesis is the result of my own investigations, and is not concurrently being submitted in candidature for any degree

Signed

Date

ACKNOWLEDGEMENTS

Firstly, I would like to thank my advisor, David Field for the guidance in the development of my Master's thesis project and for his continuous support and enthusiasm throughout the process. I would also like to thank my committee members, David Hyrenbach and Sarah-Jeanne Royer for taking time out of their busy schedules to provide insightful feedback on many aspects of this research. Much of the success of this project was due to their support.

I am incredibly grateful for all of the help that I received from volunteers both in the field and in the laboratory, especially from Tori Falk and Astrid Delorme. Astrid provided both physical and emotional support during tough days out in the field and laboratory. Tori provided generous help both processing samples and conducting neuston net tows.

Lastly, my family and friends were more than encouraging during my Master's degree, always lending an ear and words of advice when needed. I would not have been able to keep a positive outlook if it weren't for their support.

Table of Contents

Chapter 1: Microplastics in Convergence Features

Introduction

The issue of plastic accumulation in the marine environment is becoming of greater concern, prompting the scientific community to consider new methods for efficient and cost-effective removal. The input and breakdown of increasing quantities of plastic marine debris increases the rate at which microplastics (< 5 mm) are created, and the concentration of microplastics is increasing at an exponential rate in large-scale (> 200 km) convergence zones (Lebreton et al. 2018). A more well-known example of a convergence zone is the Great Pacific Garbage Patch (GPGP), which increased in microplastic mass concentration from an average of 0.4 kg/km² in the 1970s to an average of 1.23 kg/km² in 2015 (Lebreton et al. 2018). Many studies focus on this particularly large area where much of the debris in the Pacific Ocean accumulates (Law et al. 2014; Lebreton et al. 2018; Egger et al. 2020). Here, microplastics have recently been reported in concentrations of up to 3.8 pieces of plastic/m² but are most frequently in the range of 0.05 - 0.2 pieces/m² (Egger et al. 2020). However, in other areas of the North Pacific, submesoscale (1-10 km) convergence features such as internal wave-driven features have been associated with an even higher concentration of up to 70 pieces of plastic/m², but are not as well studied (Gove et al. 2019). Furthermore, debris accumulation data in smaller nearshore convergence features on the order of meters are even more scarcely mentioned in the literature (Cozar et al. 2021; de Haan et al. 2022).

Due to a combination of hydrodynamic factors, coastal topography, surface currents, tidal cycles, bathymetric features, and wind patterns, waters within 1 km of the coastline have the potential to concentrate debris up to several orders of magnitude greater than in offshore waters (Ruiz et al. 2020; Compa et al. 2020; Figure 1). Ruiz et al. (2020) collected 14 tons of floating

marine debris from 166 litter windrows within months. This debris was mostly land-based macro litter due to the close proximity to a continent, while areas near subtropical gyres tend to collect more microplastics due to mechanical and photochemical degradation over time (Moret-Ferguson et al. 2010). The findings from Ruiz et al. (2020) emphasize the cost efficiency of utilizing these convergence features for debris removal. Still, few studies have successfully quantified debris in convergence areas as nearshore where ease of access could increase the cleanup efficiency. De Haan et al. (2022) conducted a unique study in which citizen scientists were asked to perform neuston net tows off the backs of their stand-up paddleboards and found similar densities of microplastics in the GPGP (Egger et al. 2020), being amongst the first studies to illustrate the efficiency of nearshore waters for cleanup.

Transport of Microplastics in Surface Waters

The physical processes determining the transport and accumulation of microplastics in large-scale ocean gyres are well documented (Van Sebille et al. 2012; Cozar et al. 2014; Lebreton et al. 2018; Egger et al. 2020), but the mechanisms behind particles exiting these large convergence zones and making it to coastlines of islands near the gyres are less clear. However, the arrival of marine debris to coastal areas likely involves variation in the surface currents that enables debris to exit the gyres (Maximenko et al. 2012). Islands and beaches near these retention and convergence zones are most subjected to the debris, where it either deposits onto beaches, becomes retained in the coastal zone, or moves on to other areas.

Once microplastics reach the coastal zone of nearby islands from the open ocean via surface currents and offshore winds, several other environmental factors may aid in their aggregation or retention. Some processes such as internal waves, density fronts, and

topographically driven fronts are known to accumulate flotsam at the surface (Gove et al. 2019; Ruiz et al. 2020; Whitney et al. 2021; Gallardo et al. 2021). Coastal rugosity, or the fractal dimension of a coastline, may increase the accumulation of marine debris and retention time in a nearshore feature (Compa et al. 2020). In the absence of these processes, windage in the open ocean and over a large surface area influences the movement of floating particles further by having a greater effect on the transport of more buoyant debris than less buoyant particles such as microplastics, which are more influenced by surface currents (Isobe et al. 2014). Once in shallow areas, such as traveling over reef environments, wave forcing becomes more influential than wind in how efficiently water is flushed out of the site, therefore influencing how much and how long water and the debris floating in it may reside in the area (Storlazzi et al. 2018). Additionally, Storlazzi et al. (2018) illustrate that higher wind speed may aid in a longer residence time due to the pinning of surface water in an embayment. If buoyant debris becomes deposited on the beach, it then has the potential to become resuspended in the swash zone - the interface between the ocean and shore - and transport down the beach in a zig-zag pattern in the presence of a longshore current (Corcoran et al. 2009).

The swash zone is the area adjacent to shore where small waves break and exacerbate mechanical degradation (Efimova et al. 2018) and may influence a unique type of convergence (Chubarenko & Stepanova 2017). The transport and residence time of microplastics and other debris in the swash zone depends largely on the upward terminal velocity, or buoyancy, of the pieces (Hinata et al. 2017). Storm events may also increase the residence time of debris within the swash zone, only increasing deposition rates after the storm ceases (Chubarenko et al. 2018). Floating microplastics are more likely to be retained in the swash zone while less buoyant debris such as smaller particles are more susceptible to being transported offshore (Hinata et al. 2017;

Kerpen et al. 2020), however, the behavior of smaller microplastic pieces is more complicated due to the continuous oscillation through the water column caused by the detachment and reattachment of sediment particles and air bubbles (Chubarenko et al. 2018).

While the physical mechanisms of surface water largely influence the concentration of plastic, the type of debris may also play a role in whether or how it is concentrated. The movement of debris that sits lower in the water column will be more influenced by currents, while the movement of larger debris that has some surface area above water level will be more influenced by wind speed and direction, which can be explained by the concept of windage and Stokes drift (Isobe et al. 2014; Trinanes et al. 2016; Maximenko et al. 2018). For instance, while relatively large and well-organized patches of organic debris such as *Sargassum* accumulate in certain areas of the subtropical North Atlantic Ocean, other types of wind-driven debris are rarely found within these patches, likely due to other debris being more influenced by windage (Ody et al. 2019). Larger features spanning up to 100 kilometers in length are more consistent with persistent currents, while smaller features (< 1 km) are largely wind-driven (Ody et al. 2019).

Finescale Convergence

The spatial dimensions of both mesoscale and submesoscale convergence features are well-established topics in oceanography (Steele 1978; Davila et al. 2021), however, there don't appear to be widely accepted terms for any features smaller than submesoscale - less than 10 km in length (Cozar et al. 2021). "Small-scale"' is typically used as a vague term for processes smaller than mesoscale, but has also been used to define features less than 1 km (Gallardo et al. 2021). More precisely, microscale and finescale are both terms that have been used in the

literature to define features or processes on scales smaller than 10 km (Owen 1989; Johnston et al. 2005; Verma et al. 2019), however microscale is mostly used for scales on the order of a few centimeters (Owen 1989). Owen (1989) defined finescale as being on the order of a few meters, while Robinson et al. (2021) gave a much wider range of 1 to 100s of meters. Alternatively, Johnston et al. (2005) defined finescale as being on the same spatial scale as the widely accepted submesoscale, and Verma et al. (2019) defined submesoscale as 0.1-10 km and implies that finescale is anything less than 100 m in length.

The term "slick" is often used to describe a linear surface manifestation of marine debris caused by a downward velocity resulting in the convergence of surface waters, however small and fine-scale features often have many different shapes, sizes and orientations (Woodson 2018; Gove et al. 2019; Smith et al. 2021). Wind speed and direction, the position of the feature relative to the coastline and wind direction can all be used to determine possible oceanic processes causing the convergence and subsequently a term for the features (Ody et al. 2019; Gallardo et al. 2021; Smith et al. 2021). A "windrow" is a general term often given to any small-scale feature less than 10 km long, however in this study, a "feature" is defined as a convergence of debris with any shape, size, and orientation.

The physical dynamics behind mesoscale and submesoscale convergence features such as density fronts are just beginning to be studied. For example, D'Asaro et al. (2018) documented how convergence features can form as whirl-like structures by deploying drifters in a 25 x 25 km area, where the drifters converged into a 60 m diameter zone after about a week. Whitney et al. (2021) studied several surface slicks on multiple days on the west side of Hawai'i Island, most of which hypothesized to be caused primarily by internal waves, where the mass of floating debris was calculated to be up to 71 times higher within the slicks than in ambient waters. Gallardo et

al. (2021) studied slicks off the island of Rapa Nui, which were hypothesized to be formed from topographically controlled fronts and internal waves, and they found plastic in densities up to 16 times greater inside slicks than in ambient waters.

Oceanic density fronts and estuarine fronts could accumulate debris at even greater magnitudes than features created by langmuir circulation and internal waves (Cozar et al. 2021). It is well established that these slicks and surface features accumulate both biological organisms and floating debris such as microplastics, likely leading to overlap between foraging species and plastic particles, which in turn enables plastic ingestion (Gove et al. 2019, Whitney et al. 2021). Plastic ingestion is widespread and has been observed in a variety of marine predators such as seabirds (Hyrenbach et al. 2017), marine mammals (Zantis et al. 2021), and fish (Markic et al. 2020). Research in progress by Caitlyn Ogbaekwe has documented this phenomenon by examining slicks in Kaneohe Bay where manta rays (*Manta birostris*) have been observed feeding on several occasions. However, there is still limited knowledge of how and why some surface convergences form. Expanding our knowledge of how these smaller-scale features form and evolve may enhance our perspective on clean-up efforts (Gove et al. 2019; Ruiz et al. 2020; Cozar et al. 2021).

Concentration Factor

Cozar et al. (2021) discussed concentration factors of phenomena at different spatial scales and for features caused by different mechanisms, and are meant to represent how strong the converging mechanisms of a particular phenomenon at a given location and time could be (Figure 1). The concentration factor (CF) is simply a ratio of the concentration of debris found within a convergence feature versus in ambient water, and has been estimated to range from 1 -

10^5 (Cozar et al. 2021). A higher concentration of debris within a feature on a particular day could result from either more debris being present in the area resulting in a higher background concentration, and/or stronger concentrating mechanisms, meaning a larger volume of water entering the site combined with a longer retention time, and has been documented by D'Asaro et al. (2018). A higher concentration inside a feature does not necessarily mean a higher CF, unless the concentration of debris in the background is similar or lower. According to estimations by Cozar et al. (2021), mechanisms behind submesoscale and small-scale convergence are capable of concentrating debris at CFs several orders of magnitude greater than mesoscale convergence features (Cozar et al. 2021). The localized phenomenon and likely sizable CFs of these features make them potential sites for efficient removal.

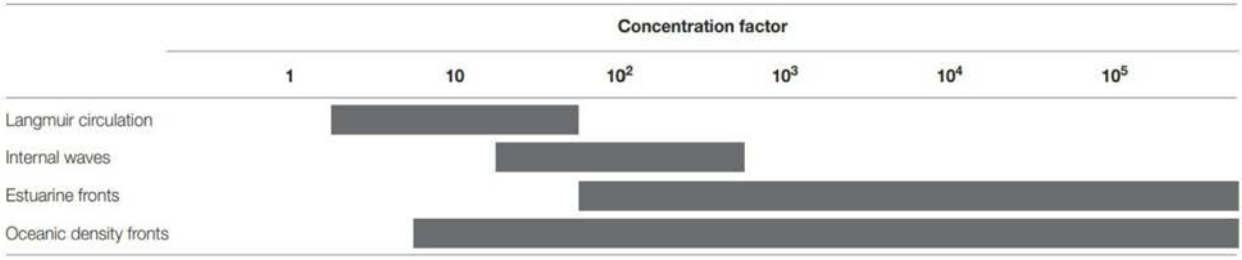

Figure 1. Range of concentration factors for features created by different physical mechanisms illustrated by Cozar et al. (2021).

The CF of different submesoscale features can illustrate how strong the converging mechanisms for that particular feature are by seeing how much debris is inside the feature versus outside (Figure 1). Inside a convergence front off the west side of the island of Hawai'i caused by internal waves, plastic concentrations up to 80 pieces/m² were found, and up to 0.1 pieces/m³ were found outside of the feature (Gove et al. 2019), resulting in the CF of 800 (Figure 1). Similarly, inside a slick caused by a density-driven front off of Northern Italy, up to 84 pieces/m² of microplastics were calculated, and less than 6 pieces/m² in outside waters, yielding a much smaller CF of 14 (Atwood et al. 2019). Inside slicks off of Easter Island caused by internal

waves, Langmuir cells, and island topography, a smaller concentration of around 16 pieces/m² were estimated (Gallardo et al. 2021). Cozar et al. (2021) calculated a range of CFs for the several aforementioned types of submesoscale concentrating mechanisms, however literature on data from smaller-scale processes to compare these with have not yet been found (Figure 1).

Convergence and Debris Accumulation in the Hawaiian Islands

The Hawaiian Islands are within close proximity to the GPGP and the subtropical convergence zone in the North Pacific (Figure 2) and are subject to the northeast trade winds (Fletcher et al. 2008), giving reason to believe that debris from the GPGP is being transported to the islands and explaining the large amounts of debris accumulating on the windward beaches and in nearshore convergence zones (Blickley et al. 2016; Brignac et al. 2019). Some studies of accumulation and clean-up efforts of marine debris in Hawai'i have focused on two main beach locations (Kahuku Beach on O'ahu and Kamilo Beach on the island of Hawai'i) with estimates of up to 5,402 pieces/m² and 9,594 pieces/m² in the top 10 and 15 cm, respectively (Young & Elliot 2016; Brignac et al. 2019; Rey et al. 2021). Both of these sites are on the windward side of their respective island, and likely accumulate large amounts of debris due to the presence and direction of the northeast trade winds, and perhaps additional circulation mechanisms resulting in high accumulation such as the geomorphological characteristics of the shores that influence physical circulation.

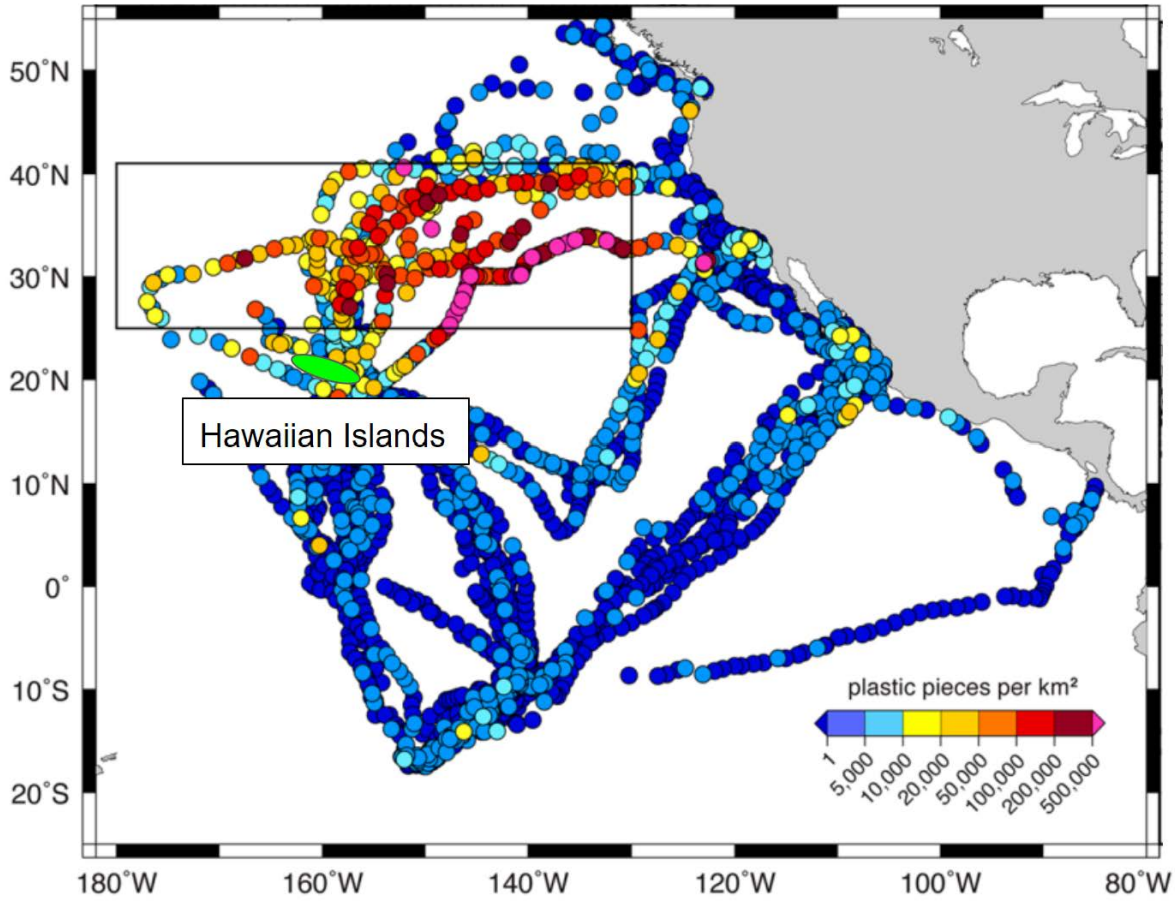

Figure 2. Figure by Law et al. (2014) illustrating densities of microplastics reported in and around the Great Pacific Garbage Patch (black box). Modified to include the relative location (size not to scale) of the main Hawaiian Islands.

At Kahuku Beach, located on the northeast side of O'ahu, another study estimated microplastic densities of > 1700 pieces/m² in the sediments, with densities within a range of ~70 - 700 pieces/m² at other locations down the windward shore of O'ahu (Rey et al. 2021). Comparably, Brignac et al. (2019) found plastic densities at Kahuku Beach to be up to five times greater than at Waimānalo Beach, and even up to twice as much as the well-known Kamilo Beach on the southeast corner of the island of Hawai'i. Furthermore, relative to beaches on the other Main Hawaiian Islands, Kahuku Beach still has been found to have the most amount of

plastic in the sediments, further emphasizing the windward sides of the islands as hotspots of microplastics (Young & Elliot 2016).

Removal Efforts

Currently, topics surrounding the best areas to target for removing surface plastic often focus on accessibility and cost effectiveness (Camins et al. 2019, Ruiz et al. 2020). Based on a model created by Sherman & van Sebille (2016), one of the most efficient generalized locations on the globe for marine debris removal is in the nearshore Northwest Pacific, particularly East Asia, where the mass flux of microplastics from land to sea is greater in concentration than in oceanic gyres. Microplastics in particular are found in densities around 15 times greater within 4 km of the coast compared with densities farther offshore (Zeri et al. 2018). The accessibility of nearshore areas allows more options for methods in which debris can be removed, such as using stand up paddleboards (SUPs) to tow a fine mesh net through the surface water to collect debris (Camins et al. 2019; De Haan et al. 2022). The ability to remove more debris in a shorter amount of time makes for efficient removal, while the easy access and lack of necessity for a vessel makes for cost-effective removal, allows for a broader scope of volunteers willing and able to help, and eliminates the use of fossil fuels. The localized phenomenon and likely sizable CFs of these finescale features make them potential sites for removal, however more needs to be understood about their cause, persistence, and frequency of occurrence in order to utilize them efficiently.

References

Atwood, E. C., Falcieri, F. M., Piehl, S., Bochow, M., Matthies, M., Franke, J., ... & Siegert, F. (2019). Coastal accumulation of microplastic particles emitted from the Po River, Northern Italy: comparing remote sensing and hydrodynamic modelling with in situ sample collections. *Marine pollution bulletin*, *138*, 561-574. https://doi.org/10.1016/j.marpolbul.2018.11.045

Blickley, L. C., Currie, J. J., & Kaufman, G. D. (2016). Trends and drivers of debris accumulation on Maui shorelines: Implications for local mitigation strategies. *Marine pollution bulletin*, *105*(1), 292-298. http://dx.doi.org/10.1016/j.marpolbul.2016.02.007

Brignac, K. C., Jung, M. R., King, C., Royer, S. J., Blickley, L., Lamson, M. R., ... & Lynch, J. M. (2019). Marine debris polymers on main Hawaiian Island beaches, sea surface, and seafloor. *Environmental science & technology*, *53*(21), 12218-12226. https://doi.org/10.1021/acs.est.9b03561

Camins, E., de Haan, W. P., Salvo, V. S., Canals, M., Raffard, A., & Sanchez-Vidal, A. (2020). Paddle surfing for science on microplastic pollution. *Science of the Total Environment*, *709*, 136178. https://doi.org/10.1016/j.scitotenv.2019.136178

Chubarenko, I., Esiukova, E., Bagaev, A., Isachenko, I., Demchenko, N., Zobkov, M., ... & Khatmullina, L. (2018). Behavior of microplastics in coastal zones. In *Microplastic contamination in aquatic environments* (pp. 175-223). Elsevier. https://doi.org/10.1016/B978-0-12-813747-5.00006-0

Chubarenko, I., & Stepanova, N. (2017). Microplastics in sea coastal zone: Lessons learned from the Baltic amber. *Environmental pollution*, *224*, 243-254. https://doi.org/10.1016/j.envpol.2017.01.085

Compa, M., Alomar, C., Mourre, B., March, D., Tintoré, J., & Deudero, S. (2020). Nearshore spatio-temporal sea surface trawls of plastic debris in the Balearic Islands. *Marine environmental research*, *158*, 104945. https://doi.org/10.1016/j.marenvres.2020.104945

Corcoran, P. L., Biesinger, M. C., & Grifi, M. (2009). Plastics and beaches: a degrading relationship. *Marine pollution bulletin*, *58*(1), 80-84. https://doi:10.1016/j.marpolbul.2008.08.022

Cózar, A., Aliani, S., Basurko, O. C., Arias, M., Isobe, A., Topouzelis, K., ... & Morales-Caselles, C. (2021). Marine litter windrows: a strategic target to understand and manage the ocean plastic pollution. *Frontiers in Marine Science*, *8*, 98. https://doi.org/10.3389/fmars.2021.571796

Cózar, A., Echevarría, F., González-Gordillo, J. I., Irigoien, X., Úbeda, B., Hernández-León, S., ... & Duarte, C. M. (2014). Plastic debris in the open ocean. *Proceedings of the National Academy of Sciences*, *111*(28), 10239-10244. http://www.pnas.org/cgi/doi/10.1073/pnas.1314705111

D'Asaro, E. A., Shcherbina, A. Y., Klymak, J. M., Molemaker, J., Novelli, G., Guigand, C. M., ... & Özgökmen, T. M. (2018). Ocean convergence and the dispersion of flotsam. *Proceedings of the National Academy of Sciences*, *115*(6), 1162-1167. http://www.pnas.org/cgi/doi/10.1073/pnas.1718453115

Davila, X., Rubio, A., Artigas, L. F., Puillat, I., Manso-Narvarte, I., Lazure, P., & Caballero, A. (2021).

Coastal submesoscale processes and their effect on phytoplankton distribution in the southeastern Bay of Biscay. *Ocean Science*, *17*(3), 849-870. https://doi.org/10.5194/os-17-849-2021

de Haan, W. P., Uviedo, O., Ballesteros, M., Canales, Í., Curto, X., Guart, M., ... & Surfing for Science Group. (2022). Floating microplastic loads in the nearshore revealed through citizen science. *Environmental Research Letters*, *17*(4), 045018. https://doi.org/10.1088/1748-9326/ac5df1

Efimova, I., Bagaeva, M., Bagaev, A., Kileso, A., & Chubarenko, I. P. (2018). Secondary microplastics generation in the sea swash zone with coarse bottom sediments: laboratory experiments. *Frontiers in Marine Science*, *5*, 313. https://doi.org/10.3389/fmars.2018.00313

Egger, M., Nijhof, R., Quiros, L., Leone, G., Royer, S. J., McWhirter, A. C., ... & Lebreton, L. (2020). A spatially variable scarcity of floating microplastics in the eastern North Pacific Ocean. *Environmental Research Letters*, *15*(11), 114056. https://doi.org/10.1088/1748-9326/abbb4f

Fletcher, C. H., Bochicchio, C., Conger, C. L., Engels, M. S., Feirstein, E. J., Frazer, N., ... & Vitousek, S. (2008). Geology of Hawaii reefs. In *Coral Reefs of the USA* (pp. 435-487). Springer, Dordrecht.

Gallardo, C., Ory, N. C., Gallardo, M. D. L. Á., Ramos, M., Bravo, L., & Thiel, M. (2021). Sea-Surface Slicks and Their Effect on the Concentration of Plastics and Zooplankton in the Coastal Waters of Rapa Nui (Easter Island). *Frontiers in Marine Science*, *8*, Art-Nr. https://doi.org/10.3389/fmars.2021.688224

Gove, J. M., Whitney, J. L., McManus, M. A., Lecky, J., Carvalho, F. C., Lynch, J. M., ... & Williams, G. J. (2019). Prey-size plastics are invading larval fish nurseries. *Proceedings of the National Academy of Sciences*, *116*(48), 24143-24149. www.pnas.org/cgi/doi/10.1073/pnas.1907496116

Hinata, H., Mori, K., Ohno, K., Miyao, Y., & Kataoka, T. (2017). An estimation of the average residence times and onshore-offshore diffusivities of beached microplastics based on the population decay of tagged meso-and macrolitter. *Marine pollution bulletin*, *122*(1-2), 17-26. https://doi.org/10.1016/j.marpolbul.2017.05.012

Isobe, A., Kubo, K., Tamura, Y., Nakashima, E., & Fujii, N. (2014). Selective transport of microplastics and mesoplastics by drifting in coastal waters. *Marine pollution bulletin*, *89*(1-2), 324-330. http://dx.doi.org/10.1016/j.marpolbul.2014.09.041

Johnston, D. W., Westgate, A. J., & Read, A. J. (2005). Effects of fine-scale oceanographic features on the distribution and movements of harbour porpoises Phocoena phocoena in the Bay of Fundy. *Marine Ecology Progress Series*, *295*, 279-293.

Kerpen, N. B., Schlurmann, T., Schendel, A., Gundlach, J., Marquard, D., & Hüpgen, M. (2020). Wave-induced distribution of microplastic in the surf zone. *Frontiers in Marine Science*, *7*, 590565. https://doi.org/10.3389/fmars.2020.590565

Law, K. L., Morét-Ferguson, S. E., Goodwin, D. S., Zettler, E. R., DeForce, E., Kukulka, T., & Proskurowski, G. (2014). Distribution of surface plastic debris in the eastern Pacific Ocean from an 11-year data set. *Environmental science & technology*, *48*(9), 4732-4738. http://dx.doi.org/10.1021/es4053076

Lebreton, L., Slat, B., Ferrari, F., Sainte-Rose, B., Aitken, J., Marthouse, R., ... & Reisser, J. (2018). Evidence that the Great Pacific Garbage Patch is rapidly accumulating plastic. *Scientific reports*, *8*(1), 1-15. https://doi.org/10.1038/s41598-018-22939-w

Maximenko, N., Hafner, J., & Niiler, P. (2012). Pathways of marine debris derived from trajectories of Lagrangian drifters. *Marine pollution bulletin*, *65*(1-3), 51-62. https://doi.org/10.1016/j.marpolbul.2011.04.016

Maximenko, N., Hafner, J., Kamachi, M., & MacFadyen, A. (2018). Numerical simulations of debris drift from the Great Japan Tsunami of 2011 and their verification with observational reports. *Marine pollution bulletin*, *132*, 5-25. https://doi.org/10.1016/j.marpolbul.2018.03.056

Morét-Ferguson, S., Law, K. L., Proskurowski, G., Murphy, E. K., Peacock, E. E., & Reddy, C. M. (2010). The size, mass, and composition of plastic debris in the western North Atlantic Ocean. *Marine Pollution Bulletin*, *60*(10), 1873-1878. https://doi.org/10.1016/j.marpolbul.2010.07.020

Ody, A., Thibaut, T., Berline, L., Changeux, T., André, J. M., Chevalier, C., ... & Ménard, F. (2019). From In Situ to satellite observations of pelagic Sargassum distribution and aggregation in the Tropical North Atlantic Ocean. *PLoS One*, *14*(9), e0222584. https://doi.org/10.1371/journal.pone.0222584

Owen, R. W. (1989). Microscale and finescale variations of small plankton in coastal and pelagic environments. *Journal of Marine Research*, *47*(1), 197-240.

Rey, S. F., Franklin, J., & Rey, S. J. (2021). Microplastic pollution on island beaches, Oahu, Hawaii. *Plos one*, *16*(2), e0247224. https://doi.org/10.1371/journal.pone.0247224

Robinson, K. L., Sponaugle, S., Luo, J. Y., Gleiber, M. R., & Cowen, R. K. (2021). Big or small, patchy all: Resolution of marine plankton patch structure at micro-to submesoscales for 36 taxa. *Science advances*, *7*(47), eabk2904. https://science.org/doi/10.1126/

Ruiz, I., Basurko, O. C., Rubio, A., Delpey, M., Granado, I., Declerck, A., ... & Cózar, A. (2020). Litter windrows in the south-east coast of the Bay of Biscay: an ocean process enabling effective active fishing for litter. *Frontiers in marine science*, *7*, 308. https://doi.org/10.3389/fmars.2020.00308

Sherman, P., & Van Sebille, E. (2016). Modeling marine surface microplastic transport to assess optimal removal locations. *Environmental Research Letters*, *11*(1), 014006. http://dx.doi.org/10.1088/1748-9326/11/1/014006

Smith, K. A., Whitney, J. L., McManus, M. A., Lecky, J., Copeland, A., Kobayashi, D. R., & Gove, J. M. (2021). Physical mechanisms driving biological accumulation in surface lines on coastal Hawaiian waters. *Continental Shelf Research*, *230*, 104558. https://doi.org/10.1016/j.csr.2021.104558

Steele, J. H. (1978). *Spatial pattern in plankton communities* (Vol. 3). Springer Science & Business Media.

Storlazzi, C. D., Cheriton, O. M., Messina, A. M., & Biggs, T. W. (2018). Meteorologic, oceanographic, and geomorphic controls on circulation and residence time in a coral

reef-lined embayment: Faga'alu Bay, American Samoa. *Coral Reefs*, *37*(2), 457-469. https://doi.org/10.1007/s00338-018-1671-4

Trinanes, J. A., Olascoaga, M. J., Goni, G. J., Maximenko, N. A., Griffin, D. A., & Hafner, J. (2016). Analysis of flight MH370 potential debris trajectories using ocean observations and numerical model results. *Journal of Operational Oceanography*, *9*(2), 126-138. https://doi.org/10.1080/1755876X.2016.1248149

Van Sebille, E., England, M. H., & Froyland, G. (2012). Origin, dynamics and evolution of ocean garbage patches from observed surface drifters. *Environmental Research Letters*, *7*(4), 044040. http://dx.doi.org/10.1088/1748-9326/7/4/044040

Verma, V., Pham, H. T., & Sarkar, S. (2019). The submesoscale, the finescale and their interaction at a mixed layer front. *Ocean Modelling*, *140*, 101400. https://doi.org/10.1016/j.ocemod.2019.05.004

Whitney, J. L., Gove, J. M., McManus, M. A., Smith, K. A., Lecky, J., Neubauer, P., ... & Asner, G. P. (2021). Surface slicks are pelagic nurseries for diverse ocean fauna. *Scientific reports*, *11*(1), 1-18. https://doi.org/10.1038/s41598-021-81407-0

Woodson, C. B. (2018). The fate and impact of internal waves in nearshore ecosystems. *Annual review of marine science*, *10*, 421-441. https://doi.org/10.1146/annurev-marine-121916-063619

Young, A. M., & Elliott, J. A. (2016). Characterization of microplastic and mesoplastic debris in sediments from Kamilo Beach and Kahuku Beach, Hawai'i. *Marine pollution bulletin*, *113*(1-2), 477-482. http://dx.doi.org/10.1016/j.marpolbul.2016.11.009

Zeri, C., Adamopoulou, A., Varezić, D. B., Fortibuoni, T., Viršek, M. K., Kržan, A., ... & Vlachogianni, T. (2018). Floating plastics in Adriatic waters (Mediterranean Sea): From the macro-to the micro-scale. *Marine Pollution Bulletin*, *136*, 341-350. https://doi.org/10.1016/j.marpolbul.2018.09.016

Chapter 2: Monitoring and Evaluating Marine Debris in a Finescale Convergence Phenomenon

Introduction

Plastic in the marine environment is a global concern, with an estimated 170 trillion pieces of plastic currently in the surface waters, primarily consisting of microplastics (< 5 mm) (Eriksen et al. 2023). This represents a three-fold increase between 1980 and 2023, and is only expected to increase as more anthropogenic debris enters the ocean and breaks up into smaller pieces (Eriksen et al. 2023). The Great Pacific Garbage Patch (GPGP) holds an estimated 1.7 trillion pieces of microplastics (0.5 - 5 mm) within the approximate 1.6 million km² of surface area, yielding an average of around 1 piece of microplastic/m² (Lebreton et al. 2018). However, densities of microplastics of up to around 4 pieces/m² inside the GPGP have recently been reported (Egger et al. 2020). The Hawaiian archipelago is located approximately 200 - 600 kilometers southwest of some of the highest reported densities of microplastics in the GPGP, with the relative proximity depending on interannual changes in basin-scale ocean dynamics (Berg et al. 2023). Therefore, plastic debris from the GPGP is presumably brought to the windward shores of islands via northeast trade winds (Blickley et al. 2016; Brignac et al. 2019), where concentrations of up to 1700 pieces/m² have been found in the upper 2 cm of sediment on windward beaches (Rey et al. 2021).

Many studies on plastic pollution focus on beach environments (Blickley et al. 2016; Brignac et al. 2019; Rey et al. 2021), however, microplastics have the potential to accumulate in nearshore submesoscale (1-10 km) surface convergence features, also considered as “coastal garbage patches” (Hajbane et al. 2021) at higher densities than in open ocean convergence zones (Wang et al. 2022). Convergence of water and floating debris can create concentrated features on

the surface of the water, which are essentially the product of two or more water masses interacting and/or subducting beneath one another (Woodson 2018). One type of submesoscale convergence called “slicks” are primarily caused by internal waves, and have been reported off the leeward side of the island of Hawai'i with microplastic concentrations 126-fold greater than concentrations in ambient waters (Gove et al. 2019). Slicks, as well as other types of convergence features, are also known to concentrate planktonic organisms and attract larval fishes, which further increases the likelihood of ingestion of microplastics by larval fishes and ultimately by higher trophic levels (Gove et al. 2019; Gallardo et al. 2021).

We have observed a nearshore concentration and retention feature at Makai Pier, southeast O’ahu, Main Hawaiian Islands, where the scale is even smaller (< 1 km) than relatively well-known submesoscale features and the mechanisms seemingly more complex. Limited studies have investigated microplastic accumulation in submesoscale convergence zones (Gove et al. 2016; Cozar et al. 2021; Gallardo et al. 2021), and to the best of our knowledge there are no published reports of a phenomenon similar to the one we have observed. At our study site, we have seen highly concentrated features of microplastics among other debris such as leaves, feathers, insects, foam, derelict fishing gear, and macroplastics with apparent concentrations that may be as high as that of oceanic density fronts and estuarine fronts under certain conditions.

One parameter that may be useful in determining the strength of convergence mechanisms for different types of features is the concentration factor (CF), a dimensionless number representing the ratio of the concentration of microplastics inside a convergence feature relative to the concentration of microplastics in ambient waters (Cozar et al. 2021). The CF can also be used to estimate the area of surface water that contributed to a concentrated feature (D’Asaro et al. 2018; Cozar et al. 2021), and investigating the relationship between various

environmental parameters and the CF may give insight into how finescale convergence features form and evolve. Additionally, because the CF is a ratio, and therefore dimensionless, it allows for order-of-magnitude comparisons across different scales and features despite materials and methods. Understanding the dynamics of finescale convergence features can improve our ability to predict the time and place of high debris concentration, which is essential for guiding debris removal efforts.

Here, we report the magnitude and variability of microplastic and organic debris densities and CFs of these finescale features by Makai Pier, and investigate how environmental conditions influence the rate and location of accumulation. Determining the magnitude of debris that can accumulate under different environmental conditions may give us a better understanding of what influences these converging mechanisms, and may enable us to apply these methods to other areas experiencing similar phenomena. The goals of this research are to predict the magnitude and locations of concentrated patches of microplastics in the surface waters, and to contribute to the knowledge gaps about the frequency, magnitude, residence times, and potential cleanup efficiency of the finescale features around the pier.

Methods

This study involved two complementary datasets; a two-year long time series of semi-quantitative surveys and quantitative surveys targeted for particular conditions (Table 1). The time series of weekly semi-quantitative observations of concentrated features of marine debris was compared with associated environmental conditions (wind strength and direction; swell height, direction and interval), while quantitative survey days focused on collecting samples of debris in the surface waters to quantify and calibrate with the semi-quantitative time

series. Quantitative sampling was opportunistically targeted for four different environmental conditions: above average north swell, above average wind speed, average wind speed, and below average wind speed.

Study Site

The Hawaiian Archipelago lies in the center of the North Pacific Ocean, just south of the GPGP, one of the largest convergence zones (Lebreton et al. 2018). The research site for this study is situated on O'ahu near the southeast corner of the island around the Makai Pier (Figure 1a). This location is exposed to the northeast trade winds which aid in the transport of debris from the GPGP to the study site and via a longshore current (Figure 1b-c).

Environmental conditions are relatively variable between days and weeks at this site, however there are some seasonal patterns worth considering for this study. During summer months (May to October), trade winds are consistent from the east-northeast (ENE) to northeast (NE) around 15-25 miles per hour, and 90% of the days experience trade wind-induced waves with periods ranging from 5-9 s and with heights between 1-3 m (Fletcher et al. 2008). Winter storms in the North Pacific bring swell from the north that ranges from 2-15 m high with a period of 14-20 s, and that north swell wraps around the island and combines with the NE trade wind waves, increasing wave height (Fletcher et al. 2008).

More localized swell and surface current activity are likely dependent on many environmental, bathymetric, and topographic features. At the end of the pier on the southeast side is a jetty around 250 ft long oriented perpendicular to the northeast trade winds, protecting the site from wind-driven energy from the northeast direction and therefore reducing wave activity within the confines of the jetty and pier (Figure 1c). A fringing reef offshore of the study

site dissipates wave energy to the area inside the jetty, however waves can be seen occasionally breaking on the southeast side of the pier over the shallow reef. Small waves also break on the narrow shore, considered the swash zone - a complex area that may often be influencing convergence (Chubarenko & Stepanova 2017). In the swash zone, microplastics and other debris may be resuspended and retained, potentially influencing the number of debris that is able to accumulate in the surface waters (Hinata et al. 2017). Unpublished data collected by undergraduate student Allyndaire Whelehan suggests that currents in the southeast direction through the site average at around 10 cm/second. The bathymetry around the pier consists of large depth gradients, where the shallow reef ranges from 0 to 5 ft in depth and the dredged area ranges from 11-20 ft in depth, and on the northwest side of the pier is a narrow, apparently naturally-formed “groovy” channel of deeper water between reefs running northwest to southeast, perpendicular to the pier (Figure 1d).

The big-picture hypothesized mechanisms for the convergence of marine debris at the pier begin with the northeast trade winds transporting surface water and debris to the eastern shore of O'ahu (Figure 1b). This onshore water transport creates a longshore flow toward the pier and/or exits via the small, naturally-forming channels in the reef. Approximately one quarter of a nautical mile southeast of the pier is Kaupo Cove, where the shoreline bends and turns to rocky headlands and where water transport may be deflected toward the pier as a countercurrent (Figure 1c). These mechanisms are hypothesized to differ in nature depending on various environmental conditions.

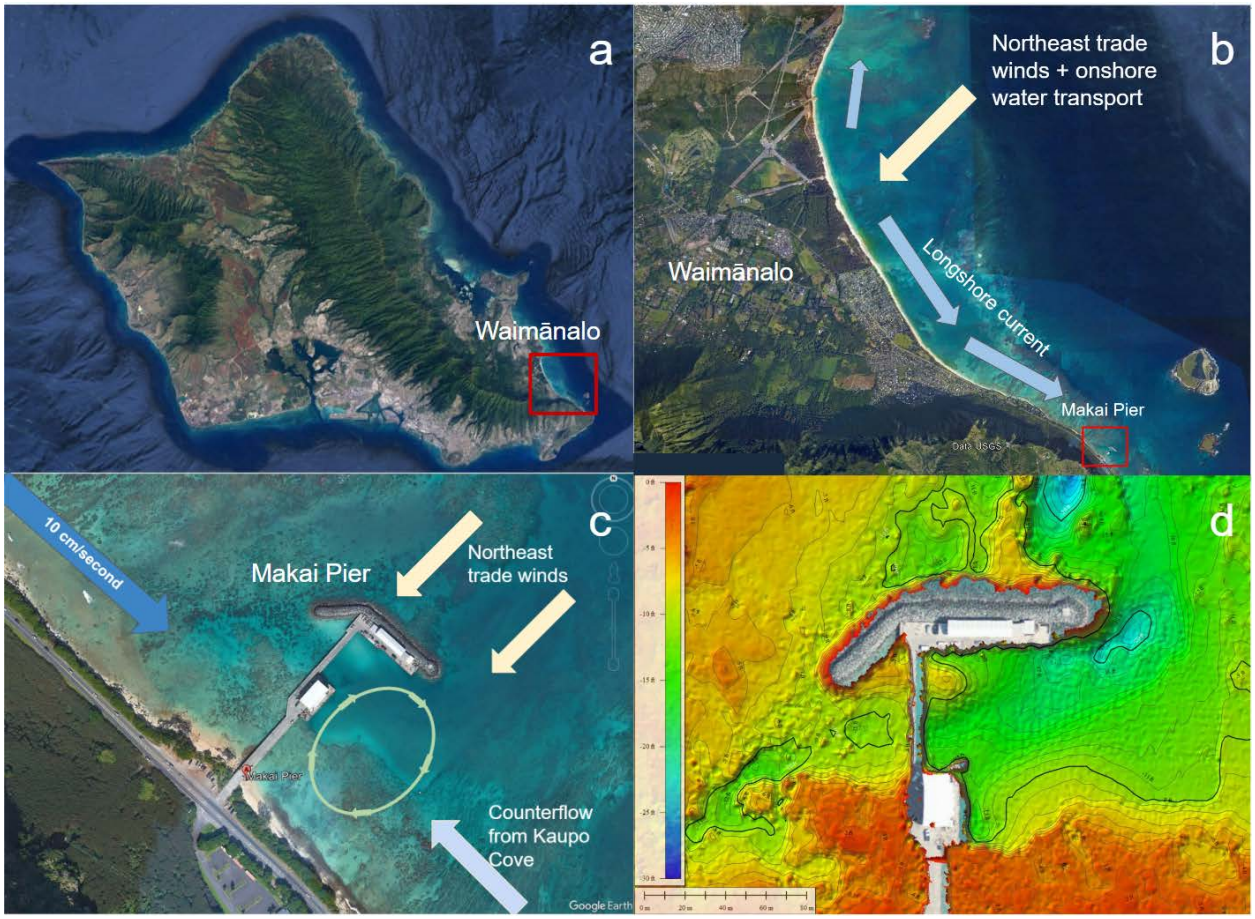

Figure 1. Environmental setting of the study area and hypothesized mechanisms that create convergence at Makai Pier. a) Map depicting relative location of Makai Pier. b) Northeast trade winds create an onshore water transport, and the interaction with the coast creates a longshore flow toward the pier, where some water escapes via small channels in the reef. c) Opposing water forcing around the pier from the longshore flow, northeast trade winds and counterflow creates convergence and/or eddy-like circulation of water. Additionally, the jetty protects the site from the northeast trade winds. d) Bathymetric map of the area around the pier. There are two areas where the bathymetry changes in depth from less than 5 ft to greater than 10 ft: northwest of the pier (left) and southeast of the pier (right). Northwest of the pier is an apparent natural "groovy" channel, and southeast of the pier is a larger dredged area. Images generated using Google Earth Pro 7.3.6.9345 (12/13/2015).

Semi-quantitative Survey Days

The purpose of the semi-quantitative surveys was to monitor order of magnitude changes in the CF of debris based on the amount and level of aggregation of different debris types in different areas around the pier, and under different environmental conditions. The weekly time series of semi-quantitative observations of debris amount and aggregation were conducted from

September 2021 to September 2023. In order to detect changes in the CF, ordinal values of 0-5 were assigned to different debris types and in different areas around the pier for both the relative amount and level of aggregation (0 referring to no debris present, 5 referring to large amounts and highly aggregated, see Table S1 for details). Here, we define concentrated "features" as areas or zones that are given a level of aggregation of three or higher, presenting any shape, orientation or size. The debris types are as follows: marine organic, terrestrial organic, feathers, bubbles/foam, line/net, microplastics, mesoplastic, macro plastics, and Portuguese man o' war (*Physalia physalis*) (see Table S1). Environmental data were obtained within 24 hours of the semi-quantitative surveys to help explain what mechanisms may be influencing this marine debris convergence phenomenon (see A.1, Figure S1).

The study site was separated into two regions north and south of the pier, each divided into designated zones for surveying, where a value for the relative amount and level of aggregation of different debris types was given to each zone (Figure 2a). There were four zones along the shore, considered the swash zone, and eight zones farther from shore that varied in depth (Figure 2a). The original time series was modified in June 2022 to include two additional survey areas northwest of the pier and two additional debris types (marine organic and mesoplastics).

Surveys were conducted by either stand up paddleboard (SUP) or surfboard, and following a predetermined pattern (Figure 2b). There were typically one to two surveyors that were consistent throughout the time series, and any debris within sight of the surveyor(s) were included in the ordinal value assigned using a dive slate. Each ordinal value of 0-5 for the estimated amount of each debris type corresponds to a range of values, while the level of aggregation refers to how concentrated the debris were, or the distance between each piece of

debris; a lower aggregation value represents pieces as spread farther apart, while a higher aggregation value represents the pieces as close to each other (within centimeters) and highly concentrated (see Table S1). If a feature (level of aggregation ≥ 3) presented with multiple debris types, the number assigned to the aggregation was that of the most highly aggregated debris type, and each feature was mapped in the ESRI Field Maps application in order to gain estimates of feature sizes (see A.1, *ESRI Field Maps Application Protocol*). Each survey – first north of the pier, then south – followed approximately the same path for the purpose of consistency, and surveys were conducted once per week between 9:00 and 17:00 (Figure 2b). An additional day per week was occasionally surveyed to target particular environmental conditions (e.g. north swell and/or days of quantitative surveys).

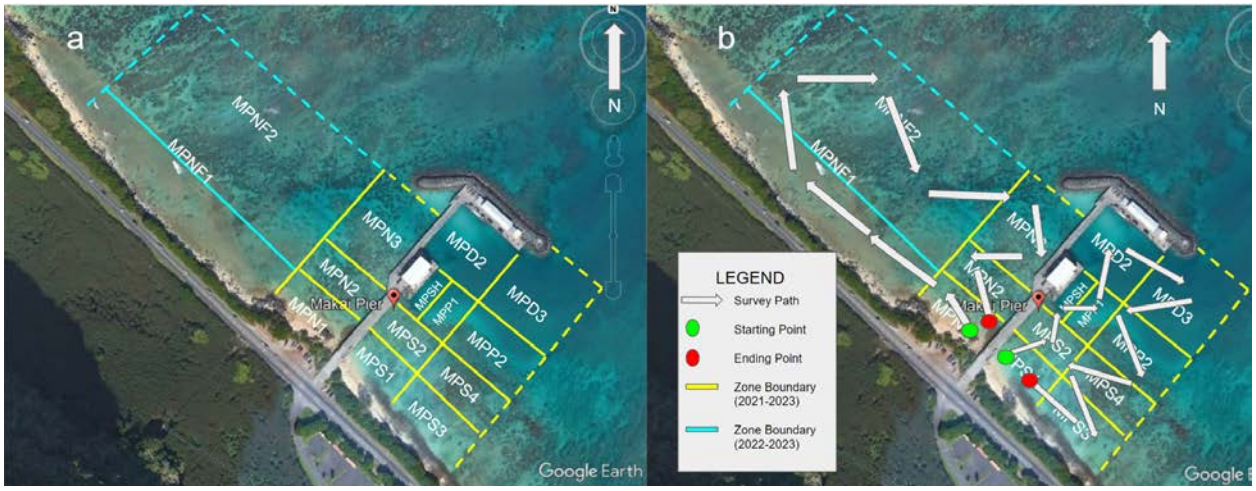

Figure 2. Map of our study site at Makai Pier exhibiting zone boundaries (yellow zones monitored since September 2021; blue zones monitored since June 2022), and approximate survey paths (white arrows) and starting and ending points of each survey (green and red dots, respectively). Zone names and abbreviations are as follows: Makai Pier North 1 (MPN1), Makai Pier North 2 (MPN2), Makai Pier North 3 (MPN3), Makai Pier North Far 1 (MPNF1), Makai Pier North Far 2 (MPNF2), Makai Pier South 1 (MPS1), Makai Pier South 3 (MPS3), Makai Pier South 4 (MPS4), Makai Pier South Hotspot (MPSH), Makai Pier Piling 1 (MPP1), Makai Pier Piling 2 (MPP2), Makai Pier Deep 2 (MPD2), and Makai Pier Deep 3 (MPD3). Satellite image was obtained from Google Maps and modified.

Environmental Variables

In order to detect any environmental influence on the occurrence and concentrations of debris at the study site, data for several environmental parameters from stations around the island of O'ahu (Figure S1) were obtained for the time and date that observations took place for each semi-quantitative survey. Data for wind speed, wind direction, wave height, wave direction, and average wave period were obtained from the National Oceanic and Atmospheric Administration's (NOAA) National Data Buoy System. Wind data were obtained from station MOKH1 in Kaneohe Bay and wave data were obtained from station 51202 off of Mokapu Peninsula (Figure S1). However, for times when this station was inactive, station 51205 located off Pauela, Maui was used, while station 51208 off Kauai was used to gain wave data from October 2021 to February 2022 due to the previous two stations both being inactive. The average value for these parameters from the six hours prior to observations was recorded into the time series data sheet.

Quantitative Survey Days

In order to gain a measurable understanding of the patterns of marine debris around Makai Pier, quantitative surveys were conducted to collect samples of marine debris, targeted for four different days of each of the four categories of environmental conditions being tested:

1. Above average North swell (> 6 ft, 345 - 30 degrees, no wind criteria),
2. Above average wind speed (> 10 knots, no direction/swell criteria),
3. Average wind speed (5-10 knots, no direction/swell criteria), and
4. Below average wind speed (< 5 knots, no direction/swell criteria).

Quantitative surveys were based on three neuston tows (330 µm mesh net, 0.99 m in width, 0.5 m height with 0.21 m below surface) that began with a semi-quantitative survey in order to identify concentrated features for sampling, where areas with an assigned aggregation of

three or higher were considered as “features” and mapped in the Field Maps app. Neuston tows were conducted through the most highly concentrated feature (referred to as the “feature tow”), through the swash zone (one of the zones directly adjacent to the beach), and through a zone away from any concentrated features (referred to as the “background tow”). However, if no concentrated feature was present, a “swash zone feature tow” was conducted in addition to the swash zone tow through the swash zone with the highest apparent concentration of microplastics.

The feature tows were typically less than one minute in length, with duration depending on the apparent concentration of debris. Background tows were typically four minutes in duration and targeted for the side of the pier which water flow appeared to be moving from in order to estimate the density of debris entering the concentrated features. Swash zone tows were typically conducted on the same side of the pier as the background tow and typically two to three minutes in duration.

In order to ultimately estimate the tow distance, one person on a surfboard or SUP recorded the time and flow meter readings at the beginning and end of each tow and mapped the towpath in the Field Maps app, while another person on a SUP steered the net. After each tow, the net was brought to shore or to an offsite location and rinsed thoroughly before adding to a labeled sample container. Any debris with a maximum length that was larger than the height or width of the sample container was rinsed and quantified on the data sheet before setting aside.

Sieve samples were occasionally collected during above average wind and north swell conditions through the surface of the water inside concentrated features that presented a level of aggregation of microplastics of 4 or higher. In order to estimate the variation of densities within concentrated patches, two sieve samples were collected from inside the densest patches of the

feature, and two sieve samples were collected from less concentrated patches within the feature, often around the perimeter of the feature.

Sample Processing

After collection, samples were processed and quantified by returning them to the laboratory and separating by size. Line/net, mesoplastics, macroplastics and all organic debris larger than 2 cm were removed and quantified. Both organic debris and microplastic petri dishes were dried in an oven at 95 degrees Fahrenheit for at least 24 hours, or air dried for at least three days, before quantifying the mass (± 0.001) on a Denver Instrument APX 200 scale (0.0001 g resolution). In order to gain information on size and polymer types, the remaining samples were sieved at 0.5 mm, then transferred to labeled plastic petri dishes using a squeeze bottle with tap water. Microplastics (> 0.5 mm) were removed and placed in a separate petri dish.

Segmentation Model

In order to quantify microplastic numbers, along with size and plastic classification data for each piece, the > 0.5 mm samples were processed using the segmentation model led by Sarah-Jeanne Royer with The Ocean Cleanup. The plastic pieces in each sample were placed on a blue photographing pad, scattered around a reference coin for size that were both provided by The Ocean Cleanup. A photo was taken from an aerial view of the photo pad with the coin and microplastics, and uploaded into the model to assign identification numbers, size and classification parameters to each piece. This same protocol was repeated with the sorted > 0.5 mm organic debris from the corresponding samples, however due to the organic debris often

sticking together and easily being broken up once dried, the model was only used to be a reference photo of the organic debris.

Feature Tow Samples

For highly concentrated samples, such as net tow samples from inside concentrated features, a plankton splitter was used to split the sample until approximately 100 - 200 plastic and organic particles remained before sieving. After running the > 0.5 mm pieces through the segmentation model, the largest twenty and smallest twenty microplastic pieces were analyzed for polymer type with a Thermo Scientific attenuated total reflectance-Fourier transform infrared spectroscopy (ATR-FTIR), using guidelines from Jung et al. (2018). The remaining portion of the split sample was kept in its original container with an updated label that represented the fraction of sample that was left. For less concentrated samples that did not require splitting, only microplastic count, size and classification data were obtained using the segmentation model. If unconfident about a particular piece of plastic, it was analyzed with ATR-FTIR in order to confirm the quantity of plastic particles in that sample.

Data Analysis

Density and concentration factor calculations

To estimate microplastic, microplastic mass and organic mass densities, the total estimated count and/or mass of debris within the sample was divided by the area towed (distance towed (m) x 0.99 m) or sieved (0.0324 m^2). The total estimated number of debris from split samples was calculated by multiplying the count by the inverse of the fraction of the split. The distance towed was derived by taking the difference in flowmeter readings and multiplying by

0.06, however, if the flow meter readings were apparently imprecise, the distance derived from the ESRI Field Maps app was used. The microplastic densities and microplastic mass densities were re-evaluated by subtracting the percentage of pieces that were misidentified from ATR-FTIR analysis. The CF was calculated for both the feature and the swash zone for each day sampled by dividing the density from the feature tow and swash zone tow by the density from the background tow.

Calibration of the semi-quantitative surveys with the quantitative densities

In order to compare the semi-quantitative data to predicted quantitative densities and CFs of debris for the two-year time series, the ordinal values for microplastic amount and level of aggregation given for each sampled feature were summed and plotted against the logarithm (base 10) of microplastic density (#/m²) from the feature tows that correspond to the given ordinal values. In order to ultimately calculate CFs for the rest of the time series, a quadratic regression was performed to obtain an equation to calculate microplastic densities. To calculate the "feature" density for each day of the time series, the sum of the ordinal values for microplastic amount and level of aggregation from any zone with a level of aggregation of three or greater for microplastics (or the zone with the highest level of aggregation if none were three or greater) were entered into the equation. To calculate background densities, the ordinal values for microplastic amount and aggregation from three zones farthest from the feature (typically zones that were frequently used for the background tows on quantitative survey days) were summed and entered into the equation. To obtain a single CF for each day of the time series, the feature densities were summed and divided by the average of the three background densities.

Statistical Tests

Significant differences in microplastic densities (#/m²) in concentrated features between environmental conditions were tested using a one-way Analysis of Variance (ANOVA) in R after testing assumptions for normality and homoscedasticity. To test any significant differences in microplastic densities between the background and swash zone, and in the background and swash zone between environmental variables, a two-way ANOVA was conducted in R after testing assumptions for normality and homoscedasticity. For both ANOVA tests, a Tukey's HSD Test for multiple comparisons was used to determine which groups were significantly different in microplastic densities from each other.

A multiple linear regression model was created in R in order to investigate the influence of five main environmental predictors (wind strength, wind direction, wave height, wave direction, wave period) on the CF derived from the semi-quantitative data.

Significant differences in the maximum length of microplastic pieces between the background, swash zone, and features within the study site were analyzed using a Kruskal-Wallis test in R because the assumptions for an ANOVA were not met. A Dunn's Test for multiple comparisons was conducted to determine which groups were significantly different. In order to investigate the relationship between the relative size (large or small) of the plastic pieces analyzed with the ATR-FTIR and their polymer type, a Chi-square test was performed in R.

Results

Magnitude of accumulation of microplastics and organic debris

The results of this study include quantitative estimates of debris around the pier from 16 individual days targeted for four different environmental conditions: below average wind speed

(light wind), average wind, above average wind, and above average north swell (Table 1). Neuston tow samples were collected from the background, swash zone, and from a concentrated feature on each sampling day, with additional sieve samples collected on days with especially highly concentrated features. Microplastics (0.5-5 mm) were recorded in numerical densities of up to 7,600 #/m² and mass densities up to around 60 grams/m² within concentrated features on certain days, and were frequently greater than 100 #/m² (Figure 3a). When sieve samples were collected, microplastic and organic debris densities were up to an order of magnitude greater or lower than from neuston net tow samples (Figure 3a-c). Organic mass was estimated in densities up to two-fold greater than microplastic mass, however, the patterns of densities and CFs between the three density types varied little (Figure 3). On 10/10/22 and 10/21/22, multiple features were sampled, giving a total of eight sieve samples on those days.

Table 1. Wind and wave conditions on each sampling day targeted for a particular environmental parameter.

Date	Environmental Condition	Wind Speed (knots)	Wind Direction (degrees)	Wave Height (ft)	Wave Direction (degrees)
10/10/22	North Swell	3.2	80	7.0	0
10/21/22	North Swell	6.7	100	6.2	0
4/11/23	North Swell	12.6	70	9.8	0
5/15/23	North Swell	10.7	40	7.0	0
3/24/23	Light Wind	1.5	70	5.0	70
4/21/23	Light Wind	4.2	100	3.7	50
5/12/23	Light Wind	1.7	270	5.5	0
9/4/23	Light Wind	1.5	100	4.4	80
4/7/23	Average Wind	9.9	90	5.7	70
6/16/23	Average Wind	6.2	90	5.4	60
7/3/23	Average Wind	8.1	45	5.1	70
8/30/23	Average Wind	8.9	90	5.6	70
5/24/23	Above Average Wind	12.0	60	5.8	90
6/26/23	Above Average Wind	11.6	80	7.4	80

7/19/23	Above Average Wind	15.3	70	9.0	80
9/11/23	Above Average Wind	11.0	90	6.0	90

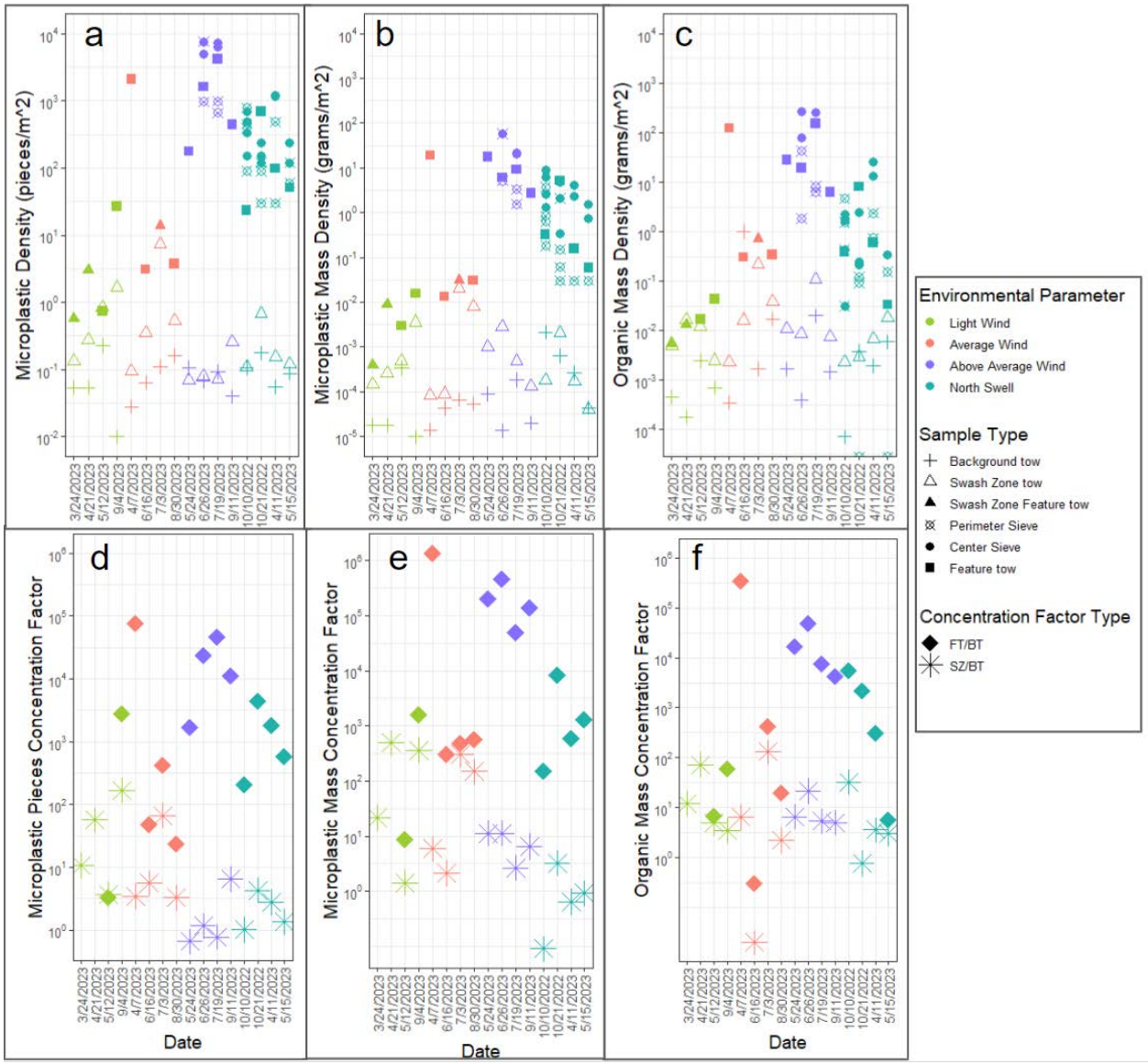

Figure 3. a) Microplastic numerical densities (#/m²), b) microplastic mass densities (grams/m²), and c) organic mass densities (grams/m²) from each sample on each quantitative survey day. Concentration factors from the feature and/or swash zone from each quantitative survey day using manta net tow densities only for d) microplastic pieces, e) microplastic mass, and f) organic debris mass. Microplastic and microplastic mass densities were adjusted based on the percentage of pieces that were confirmed as plastic from the ATR-FTIR.

Within concentrated features, microplastic and organic debris densities ranged around four orders of magnitude (Figure 3a-c). The one-way ANOVA revealed that the logarithm (base 10) of microplastic densities (#/m²) from feature tow and sieve samples were significantly different between the four environmental conditions: light wind (< 5 knots), average wind (5-10 knots), above average wind (>10 knots), and above average north swell (> 6 ft) ($p < 0.000001$; see Supplementary Data, Table S3). A Tukey's HSD Test for multiple comparisons revealed that microplastic densities (#/m²) recorded under above average wind conditions were significantly greater than densities recorded under average wind conditions ($p < 0.0005$), light wind conditions ($p < 0.00005$), and north swell conditions ($p < 0.0005$; see Supplementary Data, Table S4). Additionally, microplastic densities recorded under north swell conditions were significantly greater than densities recorded under light wind conditions ($p < 0.01$), however, there were no significant differences in microplastic densities within features between north swell and average wind conditions or between light wind and average wind conditions ($p > 0.05$; see Supplementary Data, Table S4). Within environmental conditions, the highest variability in densities lies between days under average wind conditions, where microplastic densities ranged three orders of magnitude within features (Figure 3a-c). Sieve densities typically ranged one order of magnitude within each environmental condition, however sieve samples were only collected under north swell and above average wind conditions.

Microplastic densities estimated in the swash zone and background were less variable between environmental conditions than in features, and densities in the background typically ranged around 0.02 - 0.2 #/m² with most around 0.1 #/m² (Figure 3a). Microplastic densities in the swash zone ranged from around 0.1 - 10 #/m², with an average of 0.8 #/m² - eight fold greater than the average density in the background. The two-way ANOVA revealed that microplastic

densities in the swash zone and background were significantly different (see Supplementary Data, Table S5), and a Tukey's HSD Test for multiple comparisons revealed that microplastic densities in the swash zone were significantly higher than in the background ($p < 0.005$). On some days, microplastic densities in the swash zone were similar to, or even greater than densities in features on other days under similar environmental conditions. Microplastic densities in the swash zone recorded under light wind conditions were more variable than the other environmental conditions, where densities ranged greater than an order of magnitude (Figure 3a). However, there were no significant differences found in microplastics densities from the swash zone or background between environmental conditions ($p > 0.05$; see Supplementary Data, Table S5).

Microplastic mass and organic mass densities were also typically around two to three times greater in the swash zone than in the background, with the exception of a few instances where microplastic densities in the swash zone were similar to or slightly lower (~0.002 grams/m²) than the background (Figure 3b-c). Overall, organic densities in the swash zone (0.02 grams/m² - 0.2 grams/m²) and background (0.0001grams/m² - 1 gram/m²) were much more variable than microplastic mass densities in the swash zone (0.0001 grams/m² - 0.02 grams/m²) and background (0.00001grams/m² - 0.002 grams/m²) (Figure 3a-c).

The patterns of CF for microplastic (~1 - 100,000) and organic debris (0.1 - 200,000) were less variable between environmental conditions than the densities estimated within features, and more variable between days within environmental conditions (Figure 3d-f). The highest CF for microplastic pieces was estimated to be around 75,000 on an average wind day, however for microplastic weight, the CF reached over 1,000,000. There were consistently higher CFs under north swell and above average wind conditions than other environmental parameters by around

½ order of magnitude, however some CFs recorded under light and average wind conditions were comparable.

Spatial distributions of concentrated patches during semi-quantitative and quantitative survey days

The relative sizes and locations of each sampled concentrated feature, along with their associated range of microplastic densities (#/m²) are shown in Figure 5. Most often, the more dense features were recorded under above average wind and north swell conditions, and located on the south side of the pier, near the dredged area (Figure 5). However, one sampled concentrated feature under above average wind conditions with microplastic densities ranging 100 - 1,000 #/m² occurred over the "groovy channel". Other common areas where concentrated features occurred were near the corner of the jetty and near the swash zone (Figure 5). Concentrated features recorded under light wind and average wind conditions were typically smaller in size at the time of sampling, and microplastic densities under light wind conditions only ranged from 0-100 #/m² (Figure 5).

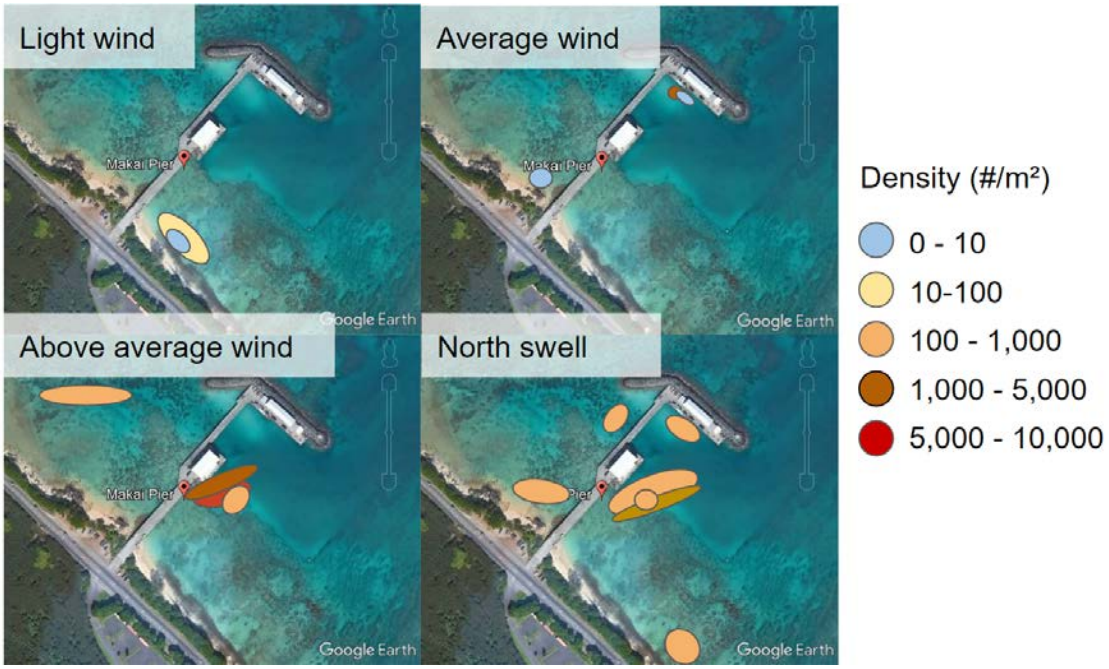

Figure 5. Ranges of microplastic densities recorded in each sampled patch, including from sieves, under each environmental condition. The sizes and shapes of the patches are relative and shown as approximations based on the location and estimated size during time of sampling.

Throughout the two-year time series, 80 quantitative surveys were conducted, and many concentrated features were observed, often occurring in and around the same zones around the study site. Several survey days showed two or more features, and some as high as seven (see Supplementary Figures, Figure S2). Out of 78 survey days, there were only eight days where no concentrated feature was observed. The distribution of percentages of the sum of the ordinal values for "amount" and "aggregation" for plastic and organic debris observed throughout the semi-quantitative surveys are compared between background zones, swash zones and hotspot zones and illustrated in Figure 8. There was typically a higher percentage of zeros in the background for both debris types than any other value, however organic debris in the swash zone showed a higher percentage (~ 15%) of larger values (2-4) than zeros (Figure 6). Hotspot zones for plastic debris exhibited about 25% more zeros than the swash zone, however there were more

frequently higher values (> 20). Organic debris exhibited similar percentage distributions between the background and hotspots (Figure 6).

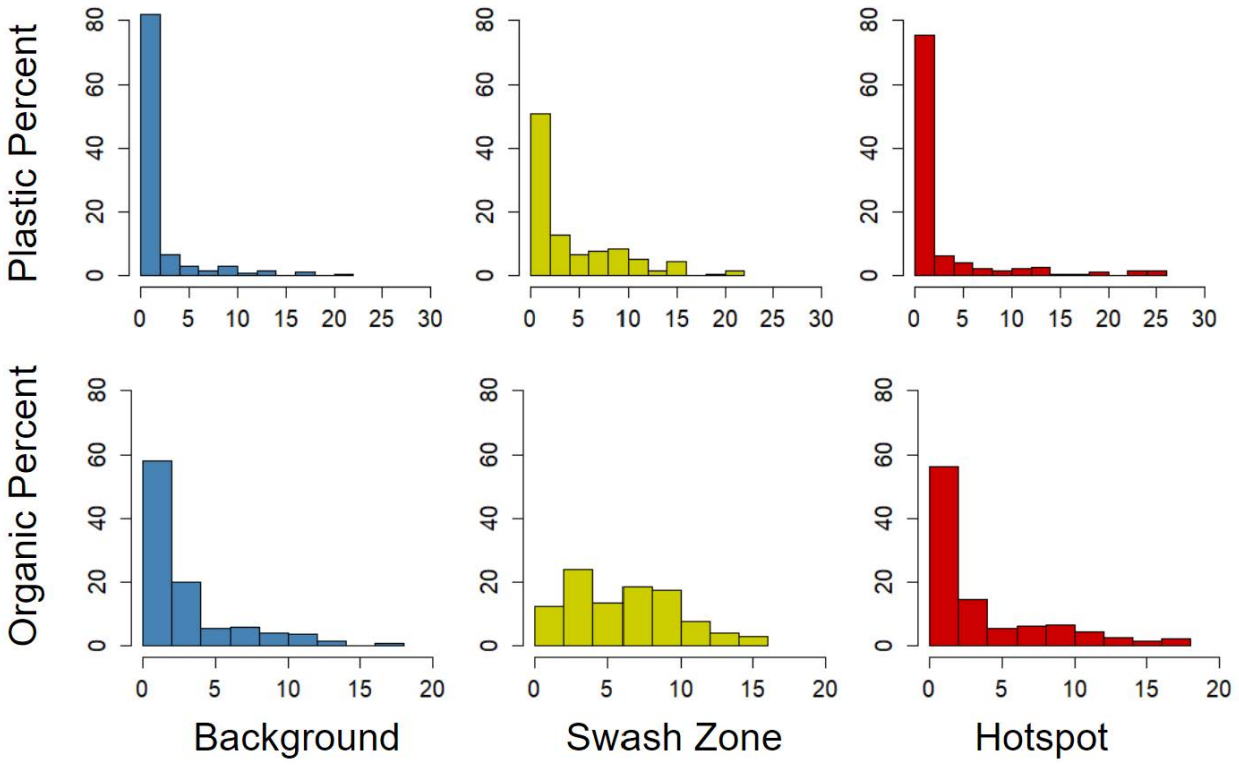

Figure 6. Percentages of the sum of ordinal values of 0-5 for the amount and level of aggregation given to plastic categories (microplastic, mesoplastic, macroplastic, line/net) and organic debris (marine and terrestrial) throughout the duration of the semi-quantitative time series in three main zones around the pier: background (MPN2, MPNF2, MPN3, MPD3, MPS4, MPP2), swash zone (MPNF1, MPN1, MPS1, MPS3), and hotspots (MPS2, MPSH, MPD2, MPP1).

Time Series of Semi-quantitative Surveys

The calibration of the semi-quantitative data with the quantitative estimates of densities resulted in a quadratic regression (Figure 7) that yielded an equation used to calculate densities and CFs for the two-year time series, as follows:

$$\log10(\text{microplastic density}) = -0.99916 + 0.13663\ x + 0.03560\ x^2$$

where x is the sum of the ordinal values of microplastic amount and level of aggregation given to the most concentrated feature during the semi-quantitative survey.

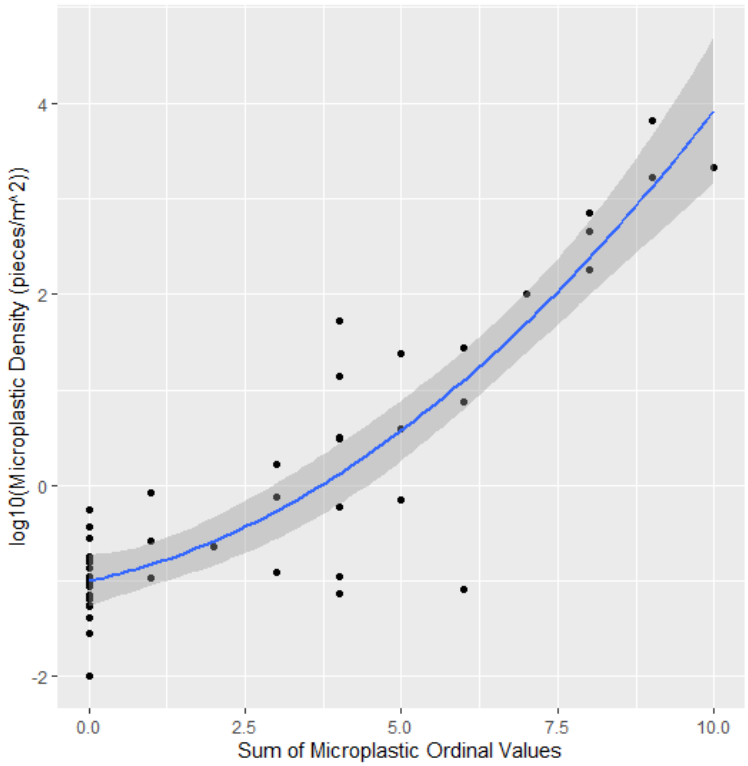

Figure 7. Quadratic regression model comparing the sum of the ordinal values for microplastic amount and aggregation with the logarithm (base 10) of estimated density of microplastics calculated from the feature for which the ordinal values were given.

Using the slope from the quadratic regression, a time series of CFs for all semi-quantitative surveys was created, exhibiting no clear seasonal patterns but reaching values of almost 100,000 (see Supplementary Figures, Figure S3). Patterns of wave height and wind strength were similar to each other (Figure S3), and both were similar to the patterns of CF (Figure S3). The overall multiple linear regression testing the influence of wind strength, wind direction, wave height, wave direction and wave period on the CF from the semi-quantitative data was significant ($R^2 = 0.26$, $F(5, 74) = 6.48$, $p < 0.00005$). Wave height was a significant predictor (= 0.23, $p < 0.05$) (Figure 8), while wind strength, wind direction, wave direction, and wave period did not significantly predict CF ($p > 0.05$).

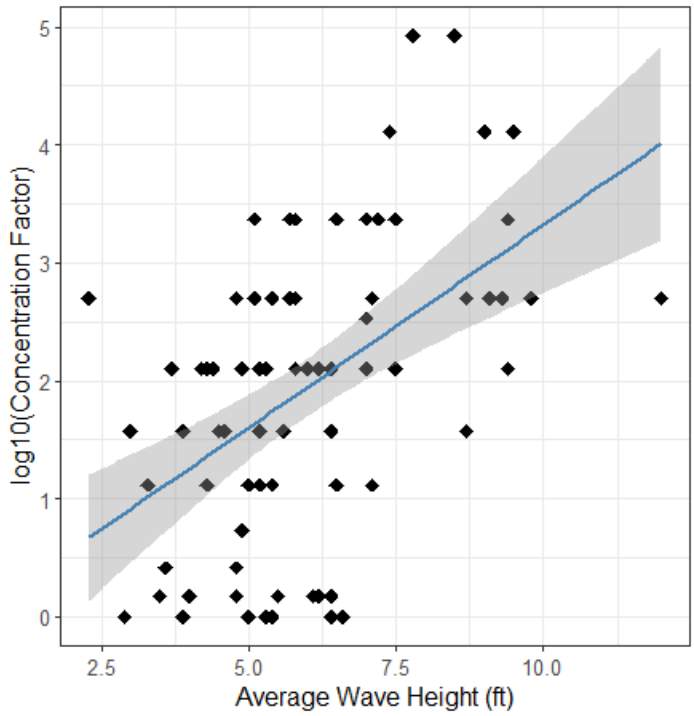

Figure 8. Relationship between average wave height (ft) and the logarithm (base 10) of the concentration factor.

Variation in plastic size, classification, and polymer type

According to the Kruskal-Wallis test investigating the difference in microplastic sizes between the background, swash zone, and features, the median maximum length (ML) of plastic pieces differed (not including line) significantly between groups (Chi-square = 55.67, df = 2, $p < 0.000005$). The ML of microplastic pieces within features were significantly greater than in the swash zone ($Z = 7.36$, $p < 0.000005$) (Figure 9), however, there were no significant differences found in the size of plastic pieces between the background and swash zone, and between the background and features ($p > 0.05$). The median ML within features was around 3.26 mm, while there were higher percentages of smaller pieces of plastic in the swash zone, and the median ML was around 2.86 mm (Figure 9).

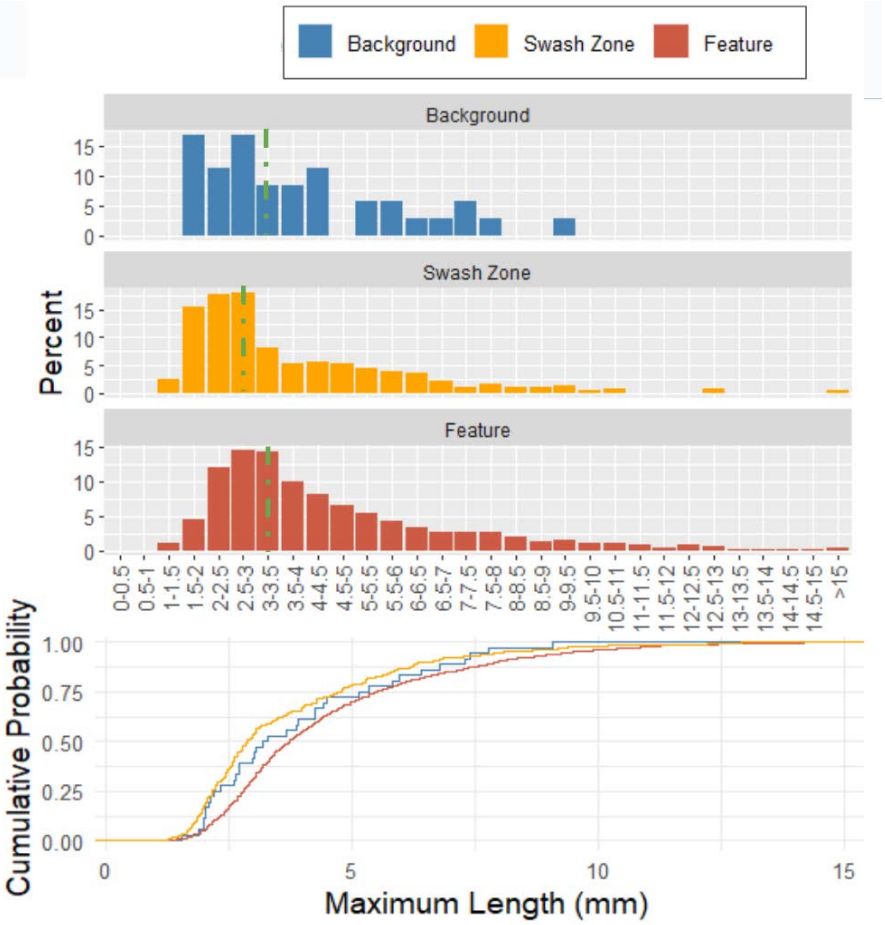

Figure 9. Distribution and cumulative probability of the maximum length (mm) of all microplastic pieces (excluding line) from the segmentation model between the background (n=36), swash zone (n=315), and features (n=2918). The green dashed line represents the median for each group.

The relative frequencies of different classifications of plastics from the segmentation model output were compared between the areas sampled and in relation to the environmental parameters (Figure 10). The relative frequency of line in the background (B) was 14% higher than in the swash zone (SZ) and 38% higher than in the features (F) (Figure 10a). The relative frequency of hard plastic pieces varied little between environmental parameters, however the relative frequency of line during above average wind (AAW) conditions was notably lower than under light wind (LW), average wind (AW), and north swell (NS) conditions (Figure 10b).

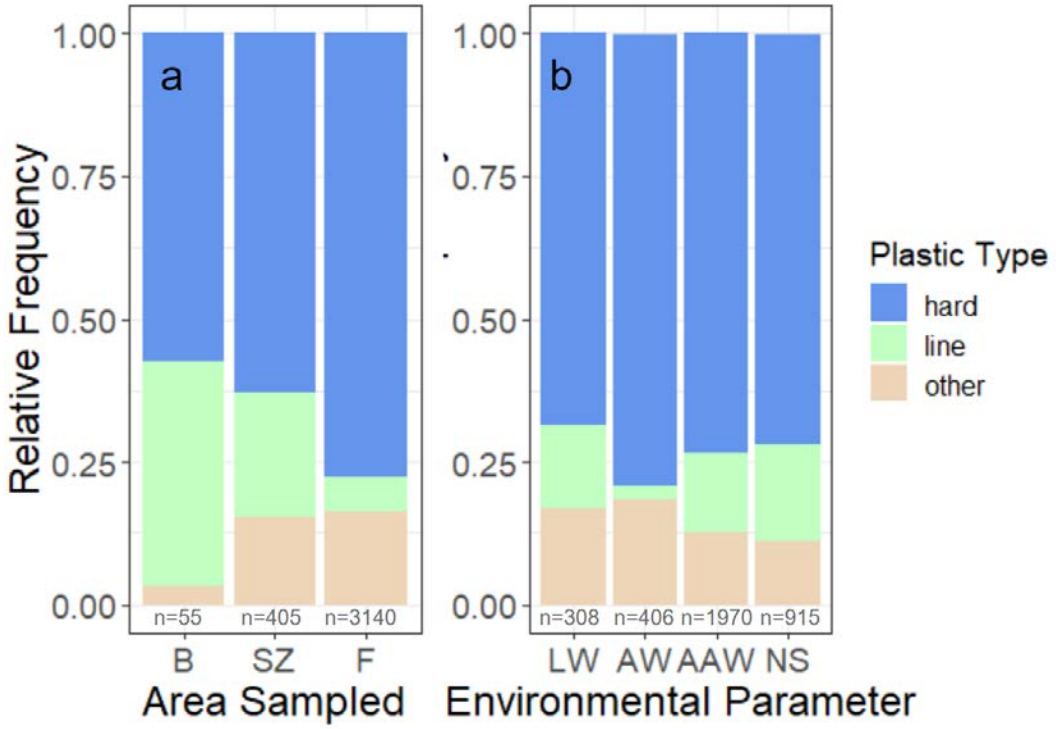

Figure 10. Relative frequencies of plastic types for all microplastic pieces run through the segmentation model. a) Plastic type relative frequencies between the background (B), swash zone (SZ) and features (F). c) Plastic type relative frequencies between light wind days (LW), average wind days (AW), above average wind days (AAW), and north swell days (NS). "Other" categories may include foam, particles, and pellets.

73.2% of plastic pieces analyzed from ATR-FTIR were identified as polyethylene (PE), while 18.1% of pieces were polypropylene (PP). This composition was relatively uniform between plastic classes, however PP made up a notably smaller percentage of pieces of line compared with other types of plastic (Figure 11a). The relative frequency of polyethylene/polypropylene mixes (PE/PP) in line was around 15% higher than in any other plastic class, and the majority of PE/PP pieces were line (Figure 11a-b). The chi-square test used to investigate the relationship between the relative size (large or small) of the plastic pieces and their polymer type suggested that PE/PP pieces are more likely to be larger pieces, while PP

pieces are more likely to be smaller (x-squared = 28.29, df = 4, $p < 0.00005$). 2.3% of pieces identified with ATR-FTIR were organic (Figure 11a) and therefore misidentified as plastic. That number was used to adjust the densities shown in Figure 3a-c, by subtracting 2.3% of the total pieces estimated per sample.

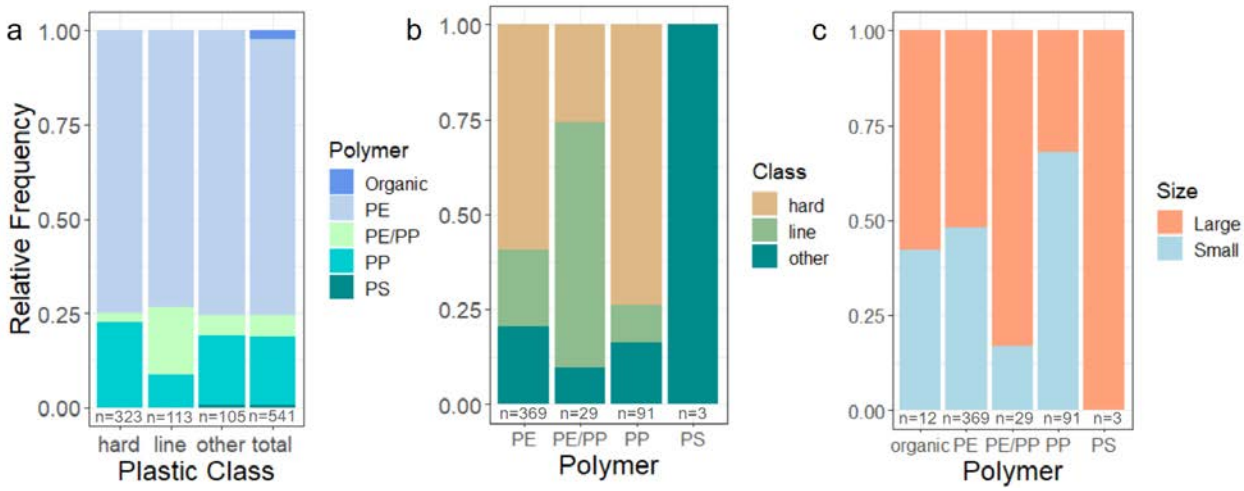

Figure 11. Plastic polymer, classification and relative size compositions of the largest twenty and smallest twenty pieces from feature net tows analyzed with ATR-FTIR. a) Relative frequencies of polymer types between different classes of microplastic detected from the segmentation model. b) Relative frequencies of different plastic classes between plastic polymers analyzed. c) Relative frequencies of relative size of microplastics subset to analyze in ATR-FTIR between polymer types identified. The plastic class "other" represents any piece not identified as being "hard" or "line" and may include pellets, particles and foam pieces.

Discussion

Overview

This study documents the ability of nearshore, finescale convergence phenomena to concentrate microplastics and other debris in concentrations, which is to the best of our knowledge, the highest concentration of microplastics in surface waters found in the literature. While microplastics and other marine debris have been reported on the windward beaches of O'ahu in concentrations of up to 5,402 pieces in the top 10 cm (Blickley et al. 2016; Brignac et

al. 2019; Rey et al. 2021), we report microplastics in a complex nearshore oceanographic phenomenon as high as 7,600 #/m² (Figure 3a). The highest microplastic concentrations reported at the pier were around three orders of magnitude greater than the highest concentrations reported in the GPGP (Figure 12a), however, caution is needed when comparing microplastic densities to the GPGP due to data from Egger et al. (2020) being from much longer net tows (30-90 min in duration) while ours were short (~30 s and/or meters in length) and sampled the most concentrated areas. Prior to this study, the highest density of microplastics recorded in the surface waters of a concentrated feature was in an estuarine front at around 1600 #/m² (Payton et al. 2020), which is still almost five-fold less than the highest microplastic densities recorded at the pier. However, unpublished documentation by Caitlyn Ogbaekwe presents microplastic densities in a submesoscale convergence feature in Kāneʻohe Bay, windward O'ahu of up to around 300 #/m², which is also located on the windward shore of O'ahu. Additionally, the estimated ranges of microplastic CFs at this finescale phenomenon are some of the highest CFs documented, and up to three orders of magnitude greater than large-scale convergence features.

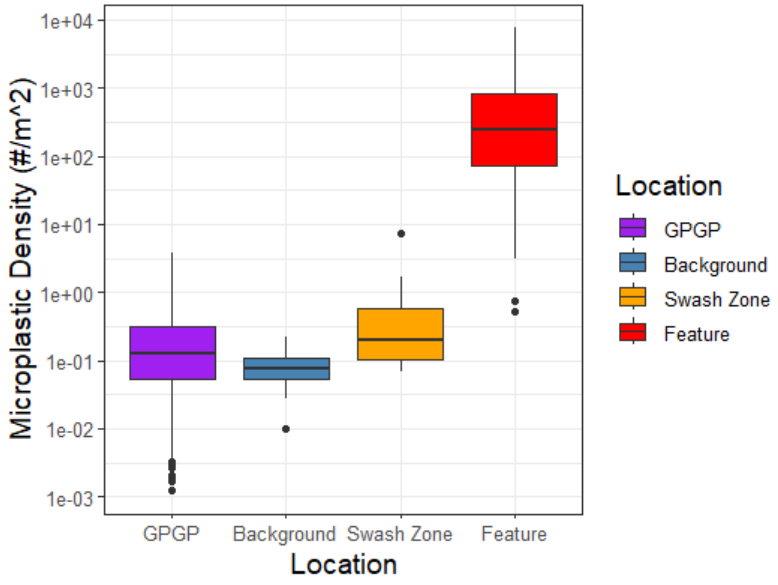

Figure 12. Comparisons of ranges of densities between the Great Pacific Garbage Patch (GPGP) in the North Pacific Ocean, and the background, swash zone, and concentrated features around Makai Pier. GPGP data are from Egger et al. (2020), and Background, Swash Zone, and Feature data are from this study.

Potential Mechanisms Behind Convergence of Debris at Makai Pier

The convergence of surface waters and floating debris around the pier likely begins with the wind-induced transport of water down the shore in a longshore current beginning at the northern end of Bellows Beach (Figure 13a). As water moves along the shore, it warms up over the reef until it meets deeper water near the pier (Figure 13b), and unpublished data by Allyndaire Whelehan suggests the water moves through the pier in the southeast direction at approximately 10 cm/second. The persistent northeast trade winds may trap surface water, and any surface debris present, within the confines of the jetty, converging with the water moving through the pier from the north (Figure 13b). With water entering the site from potentially all sides, water would have to exit via the subsurface, or from just past the jetty (Figure 13b).

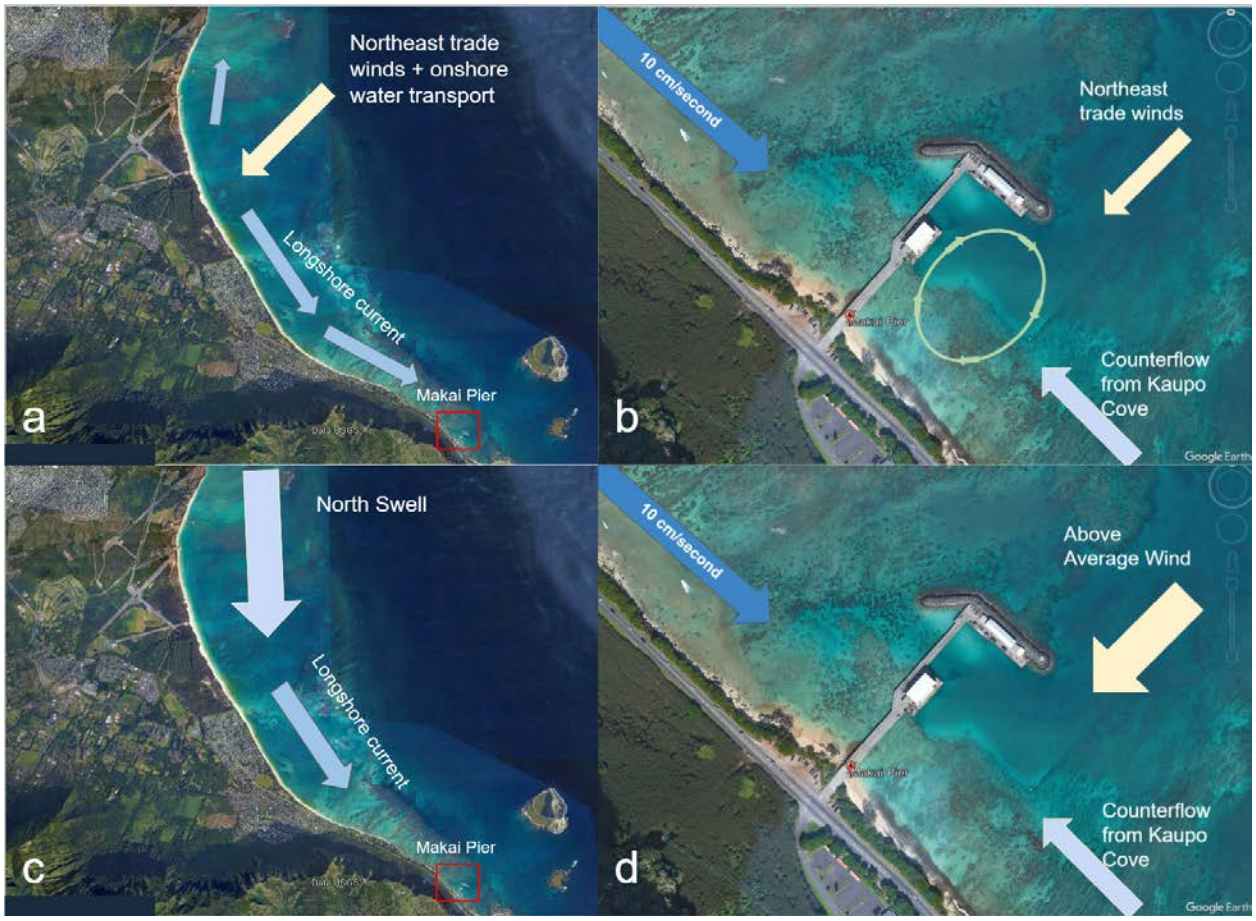

Figure 13. Potential mechanisms creating convergence of surface water and debris at Makai Pier. a) Northeast trade winds create an onshore transport of surface water, which is mostly deflected toward the southeast when it reaches the shore, toward the pier. b) Water flows through the site, on average, at about 10 cm/second in the southeast direction. The trade winds are still transporting surface water from the north east, and the addition of a potential counterflow from Kaupo Cove creates an eddy-like circulation of water. c) During a large north swell event, a larger volume of water is deflected toward the pier due to the orientation of the shore. d) Above average wind conditions further prevents debris from exiting the site. Images were generated using Google Earth Pro 7.3.6.9345 (12/13/2015).

This relatively ephemeral phenomenon has been documented to rapidly accumulate debris and evolve within a matter of hours, with several different types of features being observed. Features were typically linear in shape or elongated quasi-circular patches, and did not always contain microplastics. Some only contained organic debris and/or macro plastics and litter. Based on observations during quantitative survey days, features have at times remained in the same location and retained high concentrations of debris for at least five hours. However,

concentrated features also have often changed shape, size, level of aggregation, and/or location within a matter of one to two hours. Many times during quantitative sampling, the features changed so much that the ordinal values for amount and level of aggregation needed to be adjusted, or the feature moved to another location from the time of the semi-quantitative survey to the time of sampling. Alternatively, during light wind conditions, water moved very little within and through the study site, and debris had been observed remaining in the same location for multiple hours.

The combination of swell, wind, topography, and bathymetry make this study site and phenomenon particularly complex, as multiple factors are influencing the occurrence and persistence of concentrated features. According to the results of the multiple linear regression, wave height is the most influential environmental parameter determining the magnitude of the CF. This is likely because larger waves, especially in the north direction, exacerbate the amount of water able to flow through the pier (Storlazzi et al. 2018), therefore increasing the number of debris able to pass through and become retained. Additionally, stronger easterly to southeasterly wind speeds are favorable for higher CFs due to the pinning of surface waters in the embayment, preventing surface water and debris from exiting the site and creating a longer residence time (Storlazzi et al. 2018). The combination of the topography and northeast trade winds may also aid in a counterflow from Kaupu Cove, which may assist in an eddy-like rotation of water that has been observed during a preliminary survey day (Figure 13b), where oranges were deployed as drifters hundreds of meters apart, and within five hours converged south of the pier and made a full clockwise rotation. Fractal dimension, or coastal rugosity, has also shown to have a positive relationship with plastic abundance in nearshore areas (Compa et al. 2020), and the bathymetry around the pier creating the stark changes in depth may influence a temperature, and

therefore density gradient, which may explain the many concentrated features observed over the dredged area and groovy channel (Figure 1d; Figure 5).

The swash zone

This study is amongst the first to quantify microplastics and other debris in the swash zone and compare to nearby concentrated finescale features. While not typically as highly concentrated as other features observed around the pier, densities of microplastics within the swash zone were consistently higher than in the background (Figure 3a), and many times similar to the highest reported densities in the GPGP (Egger et al. 2020). During some quantitative sampling days, the most dense features of microplastics were located in or near the swash zone (Figure 5), and microplastics were frequently observed in the swash zone during semi-quantitative surveys (Figure 6).

The swash zone is a unique concentrating mechanism that may be collecting debris from the background, as well as contributing to concentrated features by resuspending debris from the beach. As microplastics are transported to shore by wind forcing, the beach acts as a blockade and surface currents slow down, retaining the microplastics in the swash zone. This may especially be true during storm events, when the residence time of debris within the swash zone is increased after microplastics are removed from the beach, only to be deposited once the storm ends (Chubarenko et al. 2018). Fragmentation by mechanical abrasion occurs much quicker on beaches and in the swash zone than in the open ocean (Kaandorp et al. 2021), and may even degrade plastic pieces (preferentially polyethylene) within a matter of days (Efimova et al. 2018). This generation of secondary microplastics may be further contributing to the high

concentrations, as well as the higher frequency of smaller pieces of microplastics compared with features (Figure 9).

Pieces of microplastics were significantly smaller than in features (Figure 9), and this may be due to a couple of factors. Larger pieces of plastic, and more buoyant debris in general, are more likely to be washed to the backshore of the beach, whereas smaller pieces that are less buoyant are more likely to become retained in the swash zone (Hinata et al. 2017). Additionally, the larger pieces of microplastic may be more likely to be influenced by converging mechanisms outside of the swash zone, allowing for smaller pieces to bypass the convergence and enter the swash zone, where it becomes retained.

Origin and Transport of Debris to Makai Pier

The polymer, classification and size composition of microplastic pieces found at Makai Pier suggests the potential origin of the marine debris. PE and PP polymers made up 91.3% of the detected polymers, comparable to Lebreton et al. (2018); Brignac et al. (2019); and Gove et al. (2019). This high contribution could mean that the sources of plastic in each of these studies are the same, likely the GPGP. Most of the particles in these polymer categories likely originate from fragmented packaging materials and fishing gear (Barnes et al. 2009; Kaandorp et al. 2023). Most marine debris mass in Hawai'i in particular originates from derelict fishing gear (DFG), with a large majority of arriving on the windward shores (Royer et al. 2023), and because the majority of pieces of line found at the pier were made of PE, they likely came from braided/twisted net (Corniuk et al. 2023). The idea that most microplastics in Hawai'i come from the GPGP can further be supported by the microplastic densities in the background at the pier being similar to the microplastic densities found just outside the GPGP (Figure 1).

Microplastics converged in concentrated features at the pier likely come from north of the study site (Figure 16), and the overall surface area of water contributing can be calculated using the CF. For example, a CF of 100,000 means that the area contributing to a concentrated feature is 100,000 times larger than the area of the feature itself. The logic behind this calculation is that due to the small densities in the background of the study site, the amount of water contributing to the concentrated features must be large in order to converge such high densities within a small feature.

Organic debris found in the surface waters around the pier are likely local to the area, since organic debris becomes water-logged over time and will eventually sink. However, some surveys exhibited more marine organic debris while others exhibited more terrestrial organic debris. During days under high wave conditions, marine organic debris such as algae on the reef is more likely to be torn loose and drift with the surface currents, eventually converging in a concentrated feature. On days experiencing high wind speeds and/or after a high tide, terrestrial organic debris such as leaves are more likely to be removed from land and become converged in concentrated features.

Effect of Residence Time on Microplastic Load

Using a model based on estimates of different microplastic densities in the background, the residence time of features observed throughout the surveys, and water velocity, the estimated number of pieces of microplastics becoming retained at the study site under certain conditions can be compared with the quantitative estimate of the number of pieces in a feature using the feature size and average density (see Supplementary Figures, Figure S4). When model estimates are less than quantitative estimates, it can be presumed that either the background density, water

velocity, and/or residence time are actually greater than predicted. When model estimates are greater than quantitative estimates, it can be assumed that the background density, water velocity and/or residence time are lower than predicted. Alternatively, or in addition to these different estimates, the estimated sizes of the features from the quantitative surveys may differ from reality, in which case smaller features would yield less microplastic pieces, and vice versa.

Transport of Debris Within the Study Site

The different sizes of plastics observed around the pier may be a contributing factor to how debris is concentrated, or not concentrated within features. Macro plastic was often seen concentrating in different areas than micro and meso plastic, and at times was observed moving in the opposite direction of a concentrated patch of microplastics. This may be because microplastics are considered "low-windage" items and are more likely to become retained in convergence areas such as the GPGP, while larger plastic items are considered "high-windage" (Maximenko et al. 2018). Larger pieces of hard microplastics are more likely to converge into concentrated features (Figure 9), likely because as microplastics increase in size, their rising velocity increases (Reisser et al. 2015), and if downwelling is the cause of the convergence feature, that would explain the higher percentages of larger pieces in features compared with the swash zone. Smaller particles are also more likely to remain below 0.5 m in depth according to Reisser et al. (2015), where our sampling device only went to 0.21 m in depth, meaning that the smaller pieces were not captured in our samples.

Another notable parameter that seemed to be influenced by converging mechanisms and environmental conditions was plastic classification types, mainly pieces of line (Figure 10). A higher percentage of line was found in the background than in the swash zone and features, and

if downwelling processes are in fact causing convergence, line is more susceptible to be dragged below the surface (Lee & Choi 2023) and remain at depth due to a slower rising velocity (Reisser et al. 2015). The slower rising velocity may also explain why there's a lower percentage of line under above average wind conditions than other conditions, since higher wind strength creates vertical mixing (Kukulka et al. 2012). This notion is further supported by unpublished data from net tows conducted in Kāneʻohe Bay, where pieces of line made up most of the microplastic pieces at depth, and there was much less line at the surface. Additionally, pieces with more drag, such as line, are more susceptible to be moved farther offshore (Forsberg et al. 2020), perhaps explaining the higher percentage of line in the background compared with features and the swash zone (Figure 10).

Influence of Environmental Conditions on Densities and Concentration Factors

The highest densities and some of the highest CFs were recorded under above average wind conditions, with wind direction, swell height and swell direction varying between sampling days. While the jetty prevents winds from acting on the water on the other side, wind forcing just past the jetty on the south side creates a pinning effect on the water within the confines of the pier, preventing any debris on the surface from exiting the site and increasing the residence time of debris (Figure 16d). This pinning effect is increased with an increase in wind strength, especially in the more east-southeast direction, where the wind would be able to act on the surface water within the jetty. With the increase of wind forcing on the water, as more debris enters the study site, the densities and CF of debris increase. Additionally, the protection of the jetty prevents wind-driven waves from impacting convergence features, meaning that the vertical mixing of microplastics typically caused by wind and waves does not increase with an increase

in wind strength. Interestingly, swash zone and background densities under above average wind conditions were much more similar to each other than during other conditions, and the only sampling days where the MCFs were less than one were during above average wind conditions. Perhaps the increase in water movement through and around the study site disperses debris to increase the density in the background, and another mechanism is causing the swash zone density to decrease.

If above average north swell conditions direct a larger volume of water southeastward and through the pier, a larger amount of debris also may be moving through the site (Figure 13c), and this change in swell direction and height may alter how convergence features form. During one of the north swell sampling days (4/11/23), there was a linear feature perpendicular to the beach over the large dredged area, and the water temperature on either side of the feature felt noticeably different. The water on the south side of the feature felt warmer, which is opposite of what was expected if the water coming from the shallow reef is warmer. Since swell height is directly proportional to current speeds, and current speeds tend to be higher over flat reef and slower in deep pools (Storlazzi et al. 2018), the quickly moving water may not have time to warm up. The positive correlation between swell height and current speeds also explains why swell height was the only significant parameter influencing the CF of microplastics according to the multiple linear regression performed. Therefore, the temperature gradient experienced that day may be the result of the pinning of the surface waters from the NE trade winds creating warmer water due to little water movement.

Densities and CFs recorded under light wind conditions were consistently low, while densities and CFs recorded under average wind conditions were much more variable. During light wind conditions, there is relatively little water movement through and within the study site,

suggesting that less debris is passing through the site, and more debris is presumably able to exit the site due to the lack of wind forcing that typically retains surface waters within the jetty and pier. During average wind conditions, however, the range of densities within features and in the background was much larger (Figure 3). The sampling day for which the highest CF was recorded was during average wind conditions, however, the wind strength that day was almost high enough to be considered above average (Table S2). The other three quantitative surveys under average conditions experienced similar wind strength, wind direction, wave height, wave direction, and wave period (Table S2).

Underestimations of Microplastic Densities and Concentration Factor

The exceedingly high concentrations and CFs of microplastics may in reality be even higher when considering parameters such as size limitations and processes such as vertical mixing (Kukulka et al. 2012; Reisser et al. 2015; Gunaalan et al. 2023). A recent study has concluded that up to 88% of microplastic in the surface waters may be smaller than 300 μm (Gunaalan et al. 2023); if this is true, then densities including that smaller size class class at the pier may reach over 63,000 #/m². These smaller particles are more susceptible to remain at depth, especially in rougher environmental conditions due to wind-induced mixing (Kukulka et al. 2012; Reisser et al. 2015), however, due to Makai Pier being protected from wind forcing, wind-induced mixing is unlikely to affect the surface densities of microplastics reported here, while it may impact densities reported in the GPGP. Additionally, the values for microplastic densities used for calculating CF only came from net tow samples; because microplastic densities from sieve samples were often an order of magnitude greater than densities from net tows, using the densities from sieves produces an even greater CF $> 100{,}000$ for the days in

which sieve samples were collected (Figure S5). For these reasons, microplastic CF may be more effective to report and compare between studies than microplastic densities.

Implications

Although microplastics were the focus of this study, macro plastics and derelict fishing gear were frequently found during both semi-quantitative and quantitative surveys. Items such as fishing nets, buoys, garbage bags, and even clothing were observed in the surface waters around the pier. Some macro plastic and fishing gear had been in the ocean long enough for biofouling to occur, while other items (e.g., plastic bags, food containers) were land-based.

There were many observations made during semi-quantitative surveys of interactions between marine organisms and the concentrated convergence features. On several occasions, green sea turtles (*Chelonia mydas*) were seen swimming and feeding directly underneath or around features that contained microplastics and other debris (Figure S6). Juvenile fish were occasionally observed aggregating underneath small conglomerates of net (Figure S6), and other small animals such as pufferfish, squid, and crabs were seen around concentrated features. Some pieces of plastic were even noted to have visible bite marks from a small animal (Figure S6).

Due to the accessibility, predictability, and high concentrations of debris that accumulates under certain conditions, Makai Pier may be an excellent candidate for debris removal projects. More often than not, at least one concentrated feature of either microplastics or macro litter can be observed and targeted for removal (Figure S2). For removal efforts, knowing when and where features occur is often a limiting factor (Cozar et al. 2021), however here we demonstrate that concentrated marine debris can be almost always observed at the pier during north swell and above average wind conditions, and many times during other environmental conditions. The

magnitude of CF and of pieces of debris that can be removed in a matter of minutes makes this site especially efficient as a removal site, especially considering its easy access and no need for a vessel, which also means less carbon emissions. Based on a study by Brouwer et al. (2023), immobile skimmers may be more cost-effective than mobile skimmers such as surface net tows, so understanding where debris comes from under different conditions is important to implement removal strategies. On a longer temporal scale, the estimation of interannual trends of the GPGP may be used to predict when an even higher amount of microplastics will arrive around the Hawaiian Islands (Berg et al. 2023).

Limitations

Although much was learned about the influence that different environmental conditions have on concentrated features observed at Makai Pier, some limitations should be addressed in future studies. Knowledge on the physical properties of water in and around features such as the density, current speeds and current direction under different conditions may greatly improve the predictability of concentrated features as well as other fine-scale phenomena, and monitoring these features on a longer time scale may also be beneficial in relating to the annual patterns of the GPGP (Berg et al. 2023). Tracking the water temperature during quantitative sampling would have been a helpful tool in estimating the densities of different water masses around the pier and within and around concentrated features.

While the segmentation model is a great tool to quickly measure and classify microplastics, some inaccuracies were noticed during data processing. For instance, foam was highly overestimated by the model, as only 0.6% of pieces analyzed with ATR-FTIR were identified as being polystyrene (PS), while the model detected “foam” in up to 15% of the pieces

(see Supplementary Figures, Figure S7), most of which were actually hard plastic. Some pieces were also misidentified as line, however after correcting the composition changed very little (see Supplementary Figures, Figure S8).

Conclusions

In this study, we demonstrate the impressive magnitude of microplastic densities and CFs that finescale features around Makai Pier have the ability to produce under certain conditions, particularly during above average wind and north swell conditions. Highly concentrated features preferentially converge larger pieces of microplastics compared with the swash zone, however pieces of line are less likely to become concentrated in features. Although the most dense features were located above areas with a stark change in depth, the swash zone has also consistently exhibited relatively higher concentrations of microplastics than in the background and than the average density recorded in the GPGP, operating under its own unique mechanisms.

The two-year time series demonstrates that microplastics and other marine debris are likely to be seen in the surface waters around the pier during almost any environmental condition and around 92% of the time, underscoring that this area may be an ideal candidate for targeted debris removal. An increase in wave height is likely to produce CFs of microplastics of up to 100,000, and due to the high CFs shown and little equipment needed, the results of this study demonstrates that nearshore, finescale convergence phenomena may be more efficient and less costly removal sites compared to larger, offshore convergence zones.

References

Barnes, D. K., Galgani, F., Thompson, R. C., & Barlaz, M. (2009). Accumulation and fragmentation of plastic debris in global environments. *Philosophical transactions of the royal society B: biological sciences*, *364*(1526), 1985-1998. https://doi.org/10.1098%2Frstb.2008.0205

Berg Jr, C. J., Hafner, J., Lamson, M. R., & Maximenko, N. A. (2023). The Basin-Scale Dynamics of the North Pacific Ocean Drive Interannual Variations in the Mass of Marine Debris Washing Upon Hawaiian Shores. *Available at SSRN 4504368*. https://dx.doi.org/10.2139/ssrn.4504368

Blickley, L. C., Currie, J. J., & Kaufman, G. D. (2016). Trends and drivers of debris accumulation on Maui shorelines: Implications for local mitigation strategies. *Marine pollution bulletin*, *105*(1), 292-298. http://dx.doi.org/10.1016/j.marpolbul.2016.02.007

Brouwer, R., Huang, Y., Huizenga, T., Frantzi, S., Le, T., Sandler, J., ... & Piazza, V. (2023). Assessing the performance of marine plastics cleanup technologies in Europe and North America. *Ocean & Coastal Management*, *238*, 106555. https://doi.org/10.1016/j.ocecoaman.2023.106555

Brignac, K. C., Jung, M. R., King, C., Royer, S. J., Blickley, L., Lamson, M. R., ... & Lynch, J. M. (2019). Marine debris polymers on main Hawaiian Island beaches, sea surface, and seafloor. *Environmental science & technology*, *53*(21), 12218-12226. https://doi.org/10.1021/acs.est.9b03561

Chubarenko, I., Esiukova, E., Bagaev, A., Isachenko, I., Demchenko, N., Zobkov, M., ... & Khatmullina, L. (2018). Behavior of microplastics in coastal zones. In *Microplastic contamination in aquatic environments* (pp. 175-223). Elsevier. https://doi.org/10.1016/B978-0-12-813747-5.00006-0

Compa, M., Alomar, C., Mourre, B., March, D., Tintoré, J., & Deudero, S. (2020). Nearshore spatio-temporal sea surface trawls of plastic debris in the Balearic Islands. *Marine environmental research*, *158*, 104945. https://doi.org/10.1016/j.marenvres.2020.104945

Corniuk, R. N., Shaw, K. R., McWhirter, A., Lynch IV, H. W., Royer, S. J., & Lynch, J. M. (2023). Polymer identification of floating derelict fishing gear from O'ahu, Hawai'i. *Marine Pollution Bulletin*, *196*, 115570. https://doi.org/10.1016/j.marpolbul.2023.115570

Cózar, A., Aliani, S., Basurko, O. C., Arias, M., Isobe, A., Topouzelis, K., ... & Morales-Caselles, C. (2021). Marine litter windrows: a strategic target to understand and manage the ocean plastic pollution. *Frontiers in Marine Science*, *8*, 98. https://doi.org/10.3389/fmars.2021.571796

D'Asaro, E. A., Shcherbina, A. Y., Klymak, J. M., Molemaker, J., Novelli, G., Guigand, C. M., ... & Özgökmen, T. M. (2018). Ocean convergence and the dispersion of flotsam. *Proceedings of the National Academy of Sciences*, *115*(6), 1162-1167. http://www.pnas.org/cgi/doi/10.1073/pnas.1718453115

Eriksen, M., Cowger, W., Erdle, L. M., Coffin, S., Villarrubia-Gómez, P., Moore, C. J., ... & Wilcox, C. (2023). A growing plastic smog, now estimated to be over 170 trillion plastic particles afloat in the world's oceans—Urgent solutions required. *Plos one*, *18*(3), e0281596. https://doi.org/10.1371/journal.pone.0281596

Efimova, I., Bagaeva, M., Bagaev, A., Kileso, A., & Chubarenko, I. P. (2018). Secondary microplastics

generation in the sea swash zone with coarse bottom sediments: laboratory experiments. *Frontiers in Marine Science*, *5*, 313. https://doi.org/10.3389/fmars.2018.00313

Forsberg, P. L., Sous, D., Stocchino, A., & Chemin, R. (2020). Behaviour of plastic litter in nearshore waters: First insights from wind and wave laboratory experiments. *Marine Pollution Bulletin*, *153*, 111023. https://doi.org/10.1016/j.marpolbul.2020.111023

Gallardo, C., Ory, N. C., Gallardo, M. D. L. Á., Ramos, M., Bravo, L., & Thiel, M. (2021). Sea-Surface Slicks and Their Effect on the Concentration of Plastics and Zooplankton in the Coastal Waters of Rapa Nui (Easter Island). *Frontiers in Marine Science*, *8*, Art-Nr. https://doi.org/10.3389/fmars.2021.688224

Gove, J. M., Whitney, J. L., McManus, M. A., Lecky, J., Carvalho, F. C., Lynch, J. M., ... & Williams, G. J. (2019). Prey-size plastics are invading larval fish nurseries. *Proceedings of the National Academy of Sciences*, *116*(48), 24143-24149. www.pnas.org/cgi/doi/10.1073/pnas.1907496116

Gunaalan, K., Almeda, R., Lorenz, C., Vianello, A., Iordachescu, L., Papacharalampos, K., ... & Nielsen, T. G. (2023). Abundance and distribution of microplastics in surface waters of the Kattegat/Skagerrak (Denmark). *Environmental Pollution*, *318*, 120853. https://doi.org/10.1016/j.envpol.2022.120853

Hajbane, S., Calmanovici, B., Reisser, J., Jolly, A., Summers, V., Ferrari, F., ... & Pattiaratchi, C. (2021). Coastal garbage patches: Fronts accumulate plastic films at Ashmore Reef marine park (Pulau Pasir), Australia. *Frontiers in Marine Science*, *8*, 613399. https://doi.org/10.3389/fmars.2021.613399

Hyrenbach, K. D., Hester, M. M., Adams, J., Titmus, A. J., Michael, P. A. M., Wahl, T., ... & Vanderlip, C. (2017). Plastic ingestion by Black-footed Albatross Phoebastria nigripes from Kure Atoll, Hawai'i: Linking chick diet remains and parental at-sea foraging distributions. *Marine Ornithology*, *45*, 225-236.

Isobe, A., Kubo, K., Tamura, Y., Nakashima, E., & Fujii, N. (2014). Selective transport of microplastics and mesoplastics by drifting in coastal waters. *Marine pollution bulletin*, *89*(1-2), 324-330. http://dx.doi.org/10.1016/j.marpolbul.2014.09.041

Jung, M. R., Horgen, F. D., Orski, S. V., Rodriguez, V., Beers, K. L., Balazs, G. H., ... & Lynch, J. M. (2018). Validation of ATR FT-IR to identify polymers of plastic marine debris, including those ingested by marine organisms. *Marine pollution bulletin*, *127*, 704-716. https://doi.org/10.1016/j.marpolbul.2017.12.061

Kaandorp, M. L., Dijkstra, H. A., & Van Sebille, E. (2021). Modelling size distributions of marine plastics under the influence of continuous cascading fragmentation. *Environmental Research Letters*, *16*(5), 054075. https://doi.org/10.1088/1748-9326/abe9ea

Kaandorp, M. L., Lobelle, D., Kehl, C., Dijkstra, H. A., & van Sebille, E. (2023). Global mass of buoyant marine plastics dominated by large long-lived debris. *Nature Geoscience*, 1-6. https://doi.org/10.1038/s41561-023-01216-0

Kühn, S., Booth, A. M., Sørensen, L., Van Oyen, A., & Van Franeker, J. A. (2020). Transfer of additive chemicals from marine plastic debris to the stomach oil of northern fulmars. *Frontiers in*

Environmental Science, *8*, 138. https://doi.org/10.3389/fenvs.2020.00138

Kukulka, T., Proskurowski, G., Morét‐Ferguson, S., Meyer, D. W., & Law, K. L. (2012). The effect of wind mixing on the vertical distribution of buoyant plastic debris. *Geophysical research letters*, *39*(7). http://dx.doi.org/10.1029/2012GL051116

Law, K. L., Morét-Ferguson, S. E., Goodwin, D. S., Zettler, E. R., DeForce, E., Kukulka, T., & Proskurowski, G. (2014). Distribution of surface plastic debris in the eastern Pacific Ocean from an 11-year data set. *Environmental science & technology*, *48*(9), 4732-4738. http://dx.doi.org/10.1021/es4053076

Lebreton, L., Slat, B., Ferrari, F., Sainte-Rose, B., Aitken, J., Marthouse, R., ... & Reisser, J. (2018). Evidence that the Great Pacific Garbage Patch is rapidly accumulating plastic. *Scientific reports*, *8*(1), 1-15. https://doi.org/10.1038/s41598-018-22939-w

Lee, J. H., & Choi, J. M. (2023). Measurement of Near-Surface Current Shear Using a Lagrangian Platform and Its Implication on Microplastic Dispersion. *Journal of Marine Science and Engineering*, *11*(9), 1716.

Markic, A., Gaertner, J. C., Gaertner-Mazouni, N., & Koelmans, A. A. (2020). Plastic ingestion by marine fish in the wild. *Critical Reviews in Environmental Science and Technology*, *50*(7), 657-697. https://doi.org/10.1080/10643389.2019.1631990

Maximenko, N., Hafner, J., Kamachi, M., & MacFadyen, A. (2018). Numerical simulations of debris drift from the Great Japan Tsunami of 2011 and their verification with observational reports. *Marine pollution bulletin*, *132*, 5-25. https://doi.org/10.1016/j.marpolbul.2018.03.056

Morét-Ferguson, S., Law, K. L., Proskurowski, G., Murphy, E. K., Peacock, E. E., & Reddy, C. M. (2010). The size, mass, and composition of plastic debris in the western North Atlantic Ocean. *Marine Pollution Bulletin*, *60*(10), 1873-1878. https://doi.org/10.1016/j.marpolbul.2010.07.020

Onink, V., Kaandorp, M. L., van Sebille, E., & Laufkötter, C. (2022). Influence of particle size and fragmentation on large-scale microplastic transport in the Mediterranean Sea. *Environmental science & technology*, *56*(22), 15528-15540. https://doi.org/10.1021/acs.est.2c03363

Payton, T. G., Beckingham, B. A., & Dustan, P. (2020). Microplastic exposure to zooplankton at tidal fronts in Charleston Harbor, SC USA. *Estuarine, Coastal and Shelf Science*, *232*, 106510. https://doi.org/10.1016/j.ecss.2019.106510

R Core Team (2022). R: A language and environment for statistical computing. R Foundation for Statistical Computing, Vienna, Austria. URL https://www.R-project.org/.

Reisser, J., Slat, B., Noble, K., Du Plessis, K., Epp, M., Proietti, M., ... & Pattiaratchi, C. (2015). The vertical distribution of buoyant plastics at sea: an observational study in the North Atlantic Gyre. *Biogeosciences*, *12*(4), 1249-1256. https://doi.org/10.5194/bg-12-1249-2015

Rey, S. F., Franklin, J., & Rey, S. J. (2021). Microplastic pollution on island beaches, Oahu, Hawaii. *Plos one*, *16*(2), e0247224. https://doi.org/10.1371/journal.pone.0247224

Rochman, C. M., Hoh, E., Kurobe, T., & Teh, S. J. (2013). Ingested plastic transfers hazardous chemicals to fish and induces hepatic stress. *Scientific reports*, *3*(1), 1-7. https://doi.org/10.1038/srep03263

Royer, S. J., Corniuk, R. N., McWhirter, A., Lynch IV, H. W., Pollock, K., O'Brien, K., ... & Lynch, J. M. (2023). Large floating abandoned, lost or discarded fishing gear (ALDFG) is frequent marine pollution in the Hawaiian Islands and Palmyra Atoll. *Marine Pollution Bulletin*, *196*, 115585. https://doi.org/10.1016/j.marpolbul.2023.115585

Storlazzi, C. D., Cheriton, O. M., Messina, A. M., & Biggs, T. W. (2018). Meteorologic, oceanographic, and geomorphic controls on circulation and residence time in a coral reef-lined embayment: Faga'alu Bay, American Samoa. *Coral Reefs*, *37*(2), 457-469. https://doi.org/10.1007/s00338-018-1671-4

Woodson, C. B. (2018). The fate and impact of internal waves in nearshore ecosystems. *Annual review of marine science*, *10*, 421-441. https://doi.org/10.1146/annurev-marine-121916-063619

Yamashita, R., Hiki, N., Kashiwada, F., Takada, H., Mizukawa, K., Hardesty, B. D., ... & Watanuki, Y. (2021). Plastic additives and legacy persistent organic pollutants in the preen gland oil of seabirds sampled across the globe. *Environmental Monitoring and Contaminants Research*, *1*, 97-112. https://doi.org/10.5985/emcr.20210009

Zantis, L. J., Carroll, E. L., Nelms, S. E., & Bosker, T. (2021). Marine mammals and microplastics: A systematic review and call for standardisation. *Environmental Pollution*, *269*, 116142. https://doi.org/10.1016/j.envpol.2020.116142

Appendix A

A.1. Methods

Ordinal Classification Protocol

Table S1. Ordinal classification protocol for debris amount (total particles estimated in each zone by debris type) and debris aggregation (distance between pieces at highest debris concentration) on a scale from 0 (low) to 5 (high). Each successive ordinal category represents a half order of magnitude increase in aggregation or accumulation.

Debris Type	0	1	2	3	4	5
Marine Organic	0	1-10	11-50	51-100	101-500	>500
Terrestrial Organic	0	1-5	6-10	11-20	21-50	>50
Feathers	0	1-5	6-10	11-20	21-50	>50
Bubbles	0	Very little observed, only by breaking waves	Some bubbles, (may or may not be from wave action)	Aggregation is longer-lived than wave-induced ephemeral bubbles	Large amount, distinct feature formed	Very large amount, creating film and/or higher bubbles
Line/net	0	1-5	6-10	11-20	21-50	>50
Microplastic	0	1-10	11-50	51-100	101-500	>500
Mesoplastic	0	1-10	11-50	51-100	101-500	>500
Macro plastic	0	1-5	6-10	11-20	21-50	>50
Man o war	0	1-5	6-10	11-20	21-50	>50
Aggregation for all debris types	N/A	Pieces > 3 m apart; no apparent aggregation	Pieces 1-3 m apart; some broad clustering, no distinct feature	Pieces 0.1-1 m apart; apparent feature formed with visible shape	Pieces 1-10 cm apart; highly aggregated	Pieces < 1 cm apart; extremely aggregated and debris covering surface of water

ESRI Field Maps Application Protocol

In order to monitor the locations and estimate the sizes of concentrated features, the ESRI Field Maps mobile application was used to collect location data of concentrated features during semi-quantitative surveys beginning April 2022. The map in the app was gridded the same way as shown in Figure 3, and was designed to collect points using GPS location that create polygons around concentrated features with a given debris aggregation of three or higher. A sketch of the features was first drawn out on the dive slate during the survey with estimated dimensions and later created in the app. Once the polygon was created in the app, the ordinal values were entered into a data table the same way in which they were recorded on the dive slate, and the polygon was given a title using the date in mm/dd/yy format, followed by a letter indicating succession of feature observed in alphabetical order (A, B, C, etc.). Any photos and/or videos of the feature were then added to the feature in the app.

A.2. Supplementary Data

Table S2. Environmental parameters recorded for each semi-quantitative survey, including the semi-quantitative surveys conducted before quantitative sampling. *Dates of quantitative surveys

Date	Average Wind Strength (knots)	Average Wind Direction (degrees)	Average Wave Height (ft)	Average Wave Direction (degrees)	Average Wave Period (seconds)
09/08/21	4.2	80	3.9	60	4.5
09/13/21	4.1	80	4.8	40	5.1
09/15/21	6.8	80	6.2	60	5.5
09/20/21	6.94	90	5.2	70	5.5
09/22/21	9.9	80	7.1	320	6.6
10/04/21	12	60	4.9	330	6.2
10/06/21	12	70	5.7	300	7.0
10/11/21	10	70	9.5	70	6.8
10/13/21	10	60	8.5	70	9.5
10/18/21	8	80	6.4	30	6.5
10/20/21	7	30	5.4	340	10.0
10/25/21	8	90	7.1	350	7.5
10/27/21	5.6	60	5.3	0	7.7
11/10/21	2.2	240	3.3	320	8.0

01/24/22	6.9	70	9.4	130	9.6
01/31/22	2	210	5.2	290	8.4
02/21/22	9.2	30	5.8	350	7.3
02/28/22	3.3	0	4.6	80	6.6
03/14/22	6.2	90	5.3	355	6.0
03/23/22	13.7	70	9.4	10	7.0
03/24/22	12.7	75	9.1	0	6.8
03/25/22	10.9	60	7.5	45	6.2
03/28/22	3.7	210	4.8	30	5.9
03/31/22	5.5	80	6.5	0	6.9
04/04/22	8.8	90	8.7	85	6.4
04/11/22	5.9	100	7.8	60	6.7
04/18/22	11.4	45	6.2	45	5.6
04/22/22	6.3	90	7.5	0	6.5
04/25/22	9.6	85	7.2	30	6.4
05/09/22	8	90	6.6	85	5.9
05/30/22	7.1	80	4.0	90	4.8
06/06/22	2.4	150	2.9	350	5.1
06/13/22	9	80	6.4	90	5.3
06/23/22	11.1	70	5.2	80	5.4
06/30/22	9.6	80	7.0	80	5.9
07/06/22	9	70	5.0	70	5.2
07/15/22	11.3	70	5.8	75	5.7
07/21/22	10	90	6.4	70	5.4
07/28/22	4.8	100	3.7	70	5.1
08/06/22	5.3	100	4.5	40	5.5
08/12/22	9.6	80	4.6	90	5.3
08/19/22	7.8	100	4.8	90	6.8
08/25/22	2.7	100	3.9	60	5.9
09/02/22	8.28	60	4.6	20	5.5
09/09/22	4.1	30	4.3	60	5.6
09/16/22	2.3	120	3.0	120	5.9
09/23/22	5.7	100	3.5	70	5.0
09/28/22	7.4	70	3.6	350	5.4
09/30/22	5.3	130	4.3	60	4.9
10/04/22	3.6	330	7.4	30	8.6
10/07/22	5.8	30	5.4	0	8.3
10/08/22	4.8	10	6.5	350	9.0

10/10/22*	3.2	80	7.0	0	9.7
10/14/22	3.9	330	4.9	0	8.5
10/21/22*	6.7	100	6.2	0	9.5
10/28/22	9.3	60	5.8	40	6.0
11/04/22	10.8	100	9.4	80	6.8
11/11/22	13.3	30	6.4	30	5.9
12/02/22	3.8	100	4.2	60	5.2
01/13/23	1.3	280	8.7	0	10.6
02/01/23	3.7	300	5.1	60	8.0
02/24/23	11.9	90	12.0	60	7.3
03/03/23	10.6	90	9.3	70	7.0
03/13/23	2.4	210	2.9	0	7.8
03/20/23	3.5	100	2.3	0	7.3
03/24/23*	1.5	230	5.0	70	6.6
04/03/23	6.3	100	6.1	80	5.9
04/07/23*	9.9	90	5.7	70	5.4
04/11/23*	12.6	70	9.8	0	7.4
04/21/23*	4.2	100	3.7	50	5.7
05/12/23*	1.7	30	5.5	0	7.5
05/15/23*	10.7	40	7.0	0	7.5
05/24/23*	12	60	5.8	90	5.5
06/16/23*	6.2	90	5.4	60	5.6
06/26/23*	11.6	80	7.4	80	6.1
07/03/23*	8.1	45	5.1	70	5.5
07/19/23*	15.3	70	9.0	80	6.7
08/30/23*	8.9	90	5.6	70	5.4
09/04/23*	1.5	100	4.4	80	6.6
09/11/23*	11.0	90	6.0	90	5.5

Table S3. Results of the one-way ANOVA testing the difference in mean microplastic densities in concentrated features between light wind, average wind, above average wind, and north swell conditions.

	Sum of Squares	df	Mean Square	F	P-value
Between Environmental Conditions	160.0	3	53.34	26.1	< 0.000001
Within Environmental Conditions	87.9	43	2.04	-	-
Total	247.9	46	-	-	-

Table S4. Results of Tukey's HSD Test for multiple comparisons of microplastic densities within concentrated features between light wind, average wind, above average wind, and north swell conditions.

Environmental Condition		Mean Difference	P-value	95% Confidence Interval Lower	Upper
Average Wind	Light Wind	2.29	0.1223	-0.41	4.99
Average Wind	Above Average Wind	-4.43	< 0.0001	-6.64	-2.22
Average Wind	North Swell	-2.04	0.0518	-4.08	0.01
North Swell	Light Wind	4.33	< 0.0001	2.28	6.37
North Swell	Above Average Wind	-2.40	0.0001	-3.72	-1.07
Above Average Wind	Light Wind	6.72	< 0.0001	4.51	8.93

Table S5. Results of the two-way ANOVA testing the difference in mean microplastic densities between the locations of swash zone and background tows, and between light wind, average wind, above average wind, and north swell conditions.

Source of Variation	SS	df	MS	F	p-value
Location	2.69	1	2.69	13.67	0.001
Environmental Condition	0.66	3	0.22	1.12	0.360
Interaction	1.05	3	0.35	1.79	0.180
Error	4.72	24	0.20	-	-
Total	9.13	31	-	-	-

Table S6. Results of Tukey's HSD Test for multiple comparisons of microplastic densities between the swash zone and background, and between light wind, average wind, above average wind, and north swell conditions.

Location		Mean Difference	P-value	95% Confidence Interval Lower	Upper
Swash Zone	Background	0.58	0.0011	0.26	0.90
Environmental Condition		**Mean Difference**	**P-value**	**95% Confidence Interval Lower**	**Upper**
Average Wind	Light Wind	0.14	0.9230	-0.47	0.75

Average Wind	North Swell	0.19	0.8187	-0.42	0.81
North Swell	Light Wind	-0.05	0.9945	-0.67	0.56
North Swell	Above Average Wind	0.21	0.7893	-0.41	0.82
Above Average Wind	Light Wind	-0.26	0.6463	-0.87	0.35

A.3. Supplementary Figures

Figure S1. Map of southeast O'ahu exhibiting each station location for which we collect environmental data. Station 1612480 is wind data from NOAA and Station 51202 is wave data from NOAA. Satellite image was generated using Google Earth Pro 7.3.6.9345 (12/13/2015).

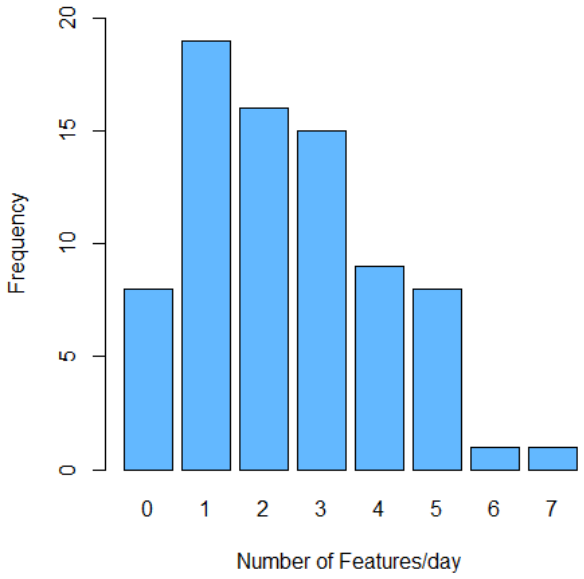

Figure S2. Histogram of the number of features observed during each semi-quantitative survey day from September 2021 - September 2023. A "feature" is defined as any area within a zone, or spanning multiple zones, that was given an ordinal value of ≥ 3 for any debris type during the semi-quantitative survey.

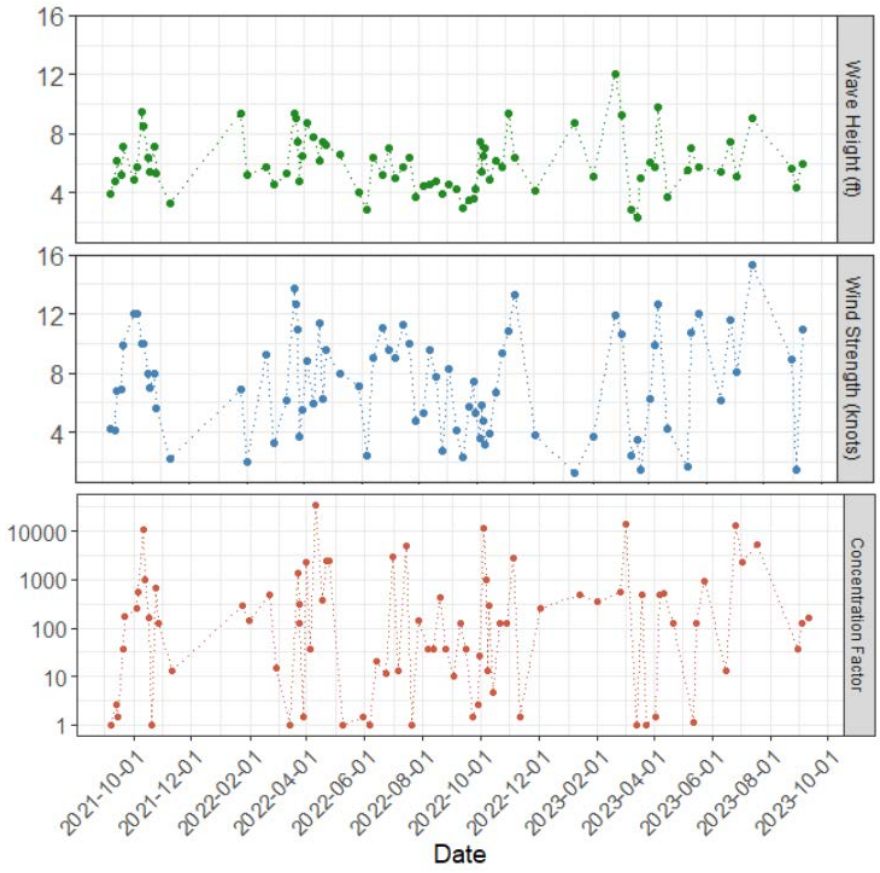

Figure S3. Time series of wind strength (green), wave height (blue) and concentration factor of microplastics calculated using the quadratic regression formula (red) from all semi-quantitative surveys. Wave height (ft) and wind strength (knots) were calculated using the average of the six hours prior to the survey.

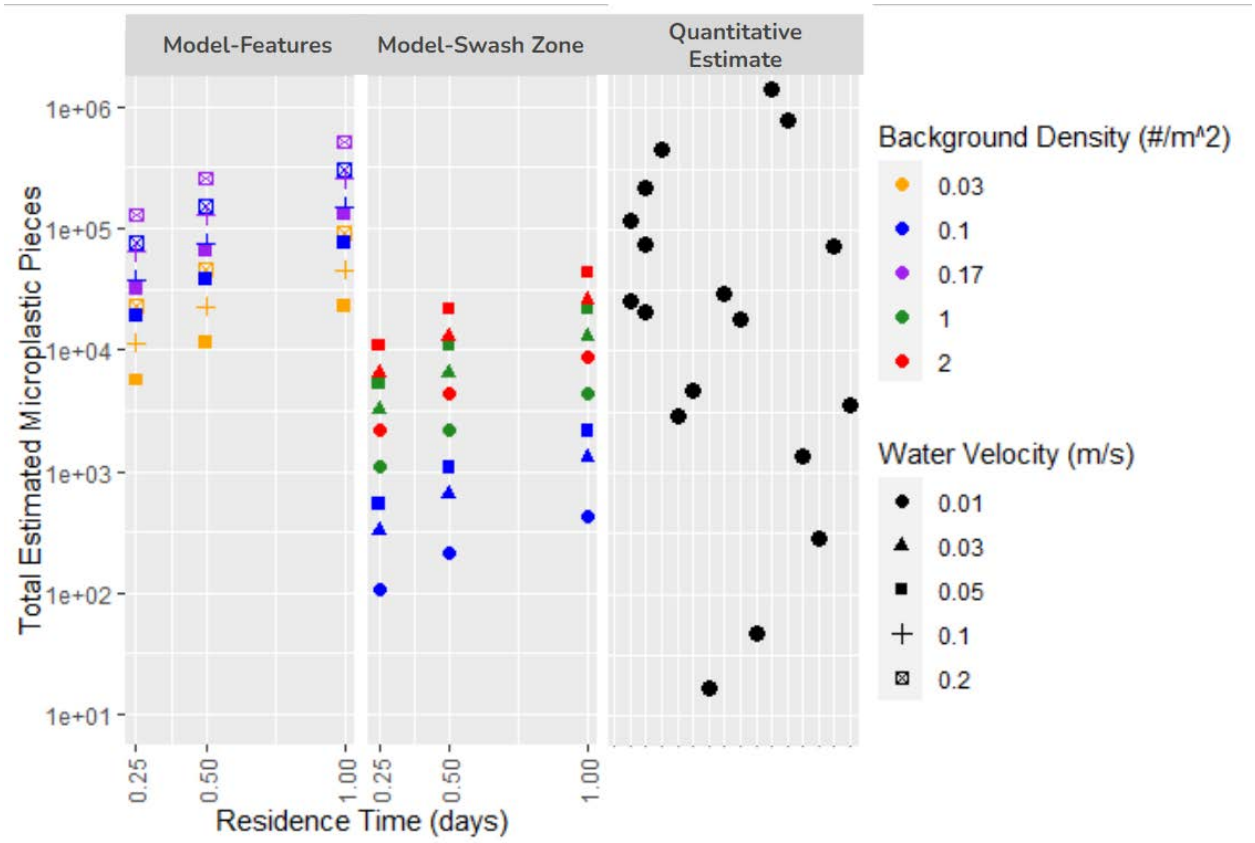

Figure S4. Estimates of total number of microplastic pieces retained at Makai Pier based on different environmental or quantitative estimates. The model estimates for features and swash zone are based on these variables: length of pier (m), seconds in a day (seconds/day), velocity (m/s), background density (pieces/m^2), and residence time (days). The quantitative estimates are based on the estimated size of features measured in the ESRI Field Maps app, and the estimate of average density recorded from net tow and/or sieve samples.

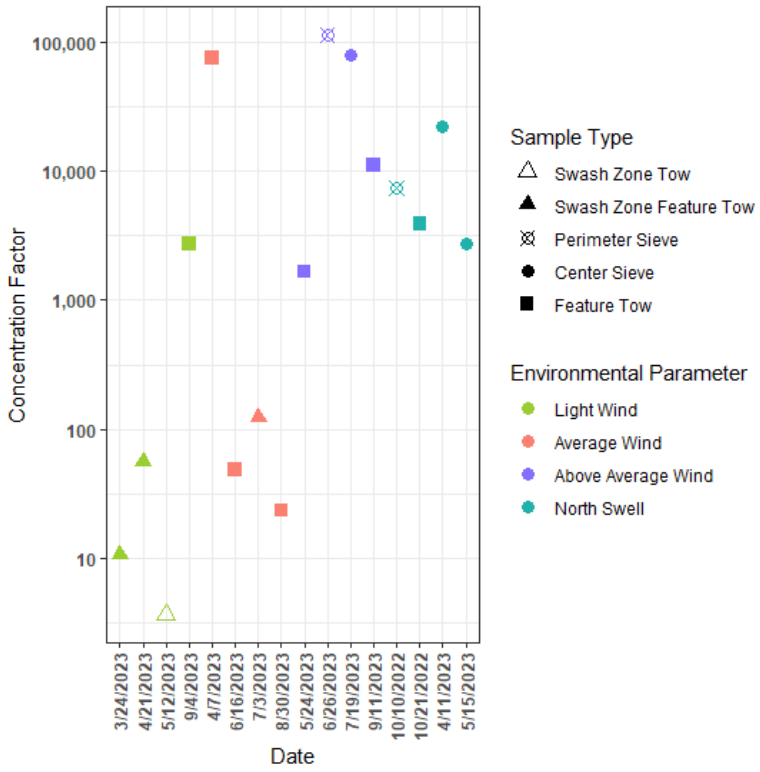

Figure S5. Concentration factors using the highest reported density on each sampling date when including sieve samples.

Figure S6. Photographs of interactions between marine organisms and marine debris and/or concentrated features. a) turtle swimming underneath feature, b) juvenile fish aggregating underneath small conglomerate of fishing net, and c) plastic piece with bites taken out of it.

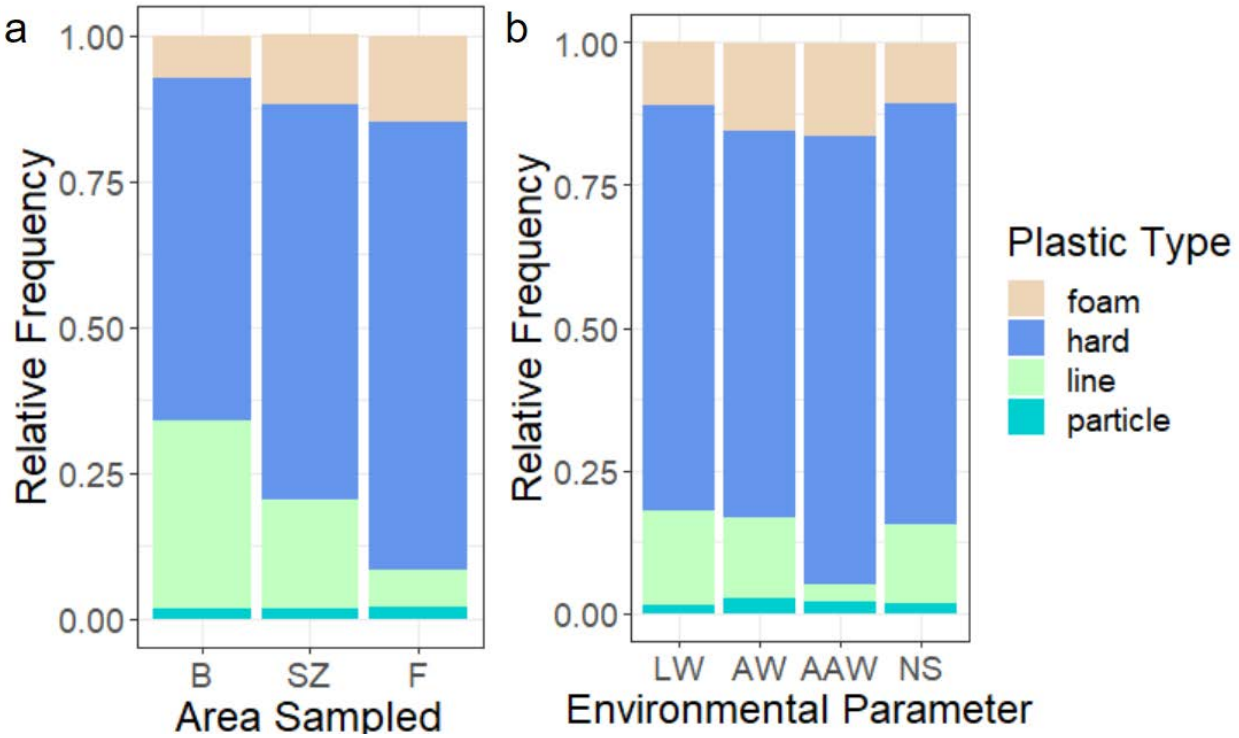

Figure S7. Relative frequencies of plastic types for all microplastic pieces run through the segmentation model. a) Plastic type relative frequencies between the background (B), swash zone (SZ) and features (F). c) Plastic type relative frequencies between light wind days (LW), average wind days (AW), above average wind days (AAW), and north swell days (NS).

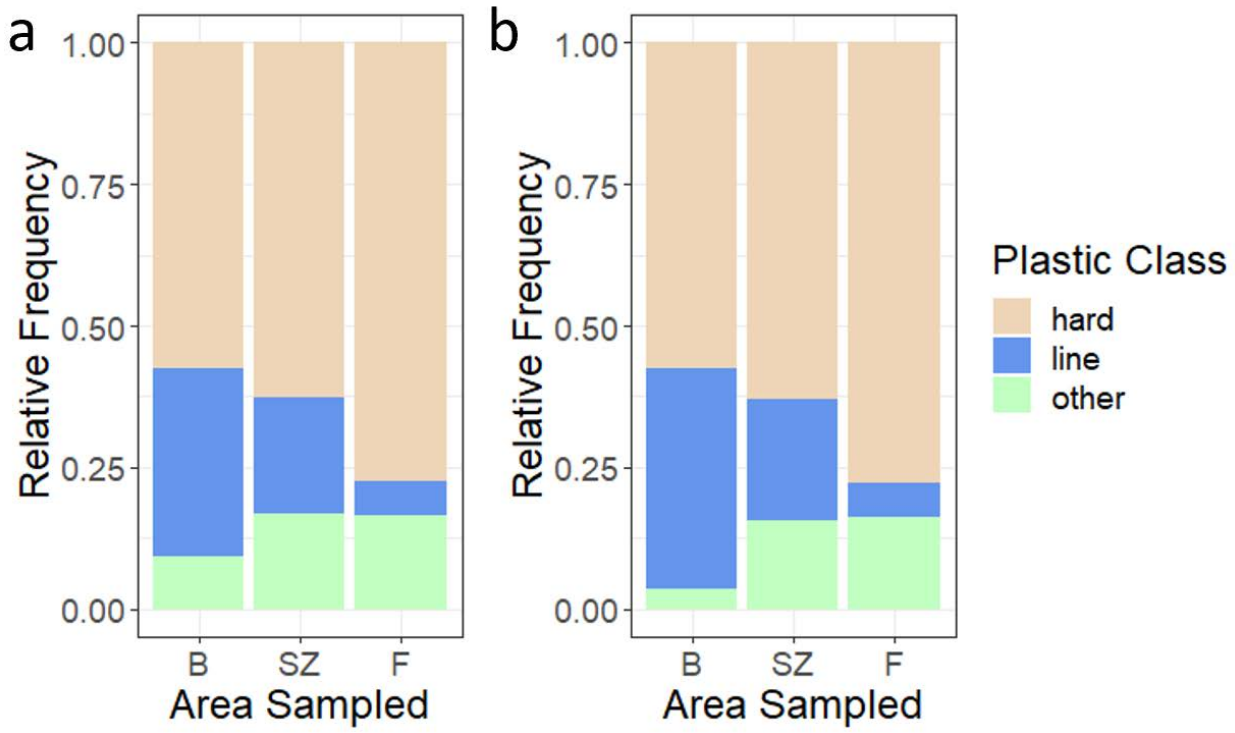

Figure S8. Relative frequencies of plastic types for all microplastic pieces run through the segmentation model between areas sampled: Background (B), swash zone (SZ) and features (F). a) Relative frequencies of plastic types before "line" were assessed from the model and re-evaluated accordingly. b) Relative frequencies of plastic types after "line" were re-evaluated.

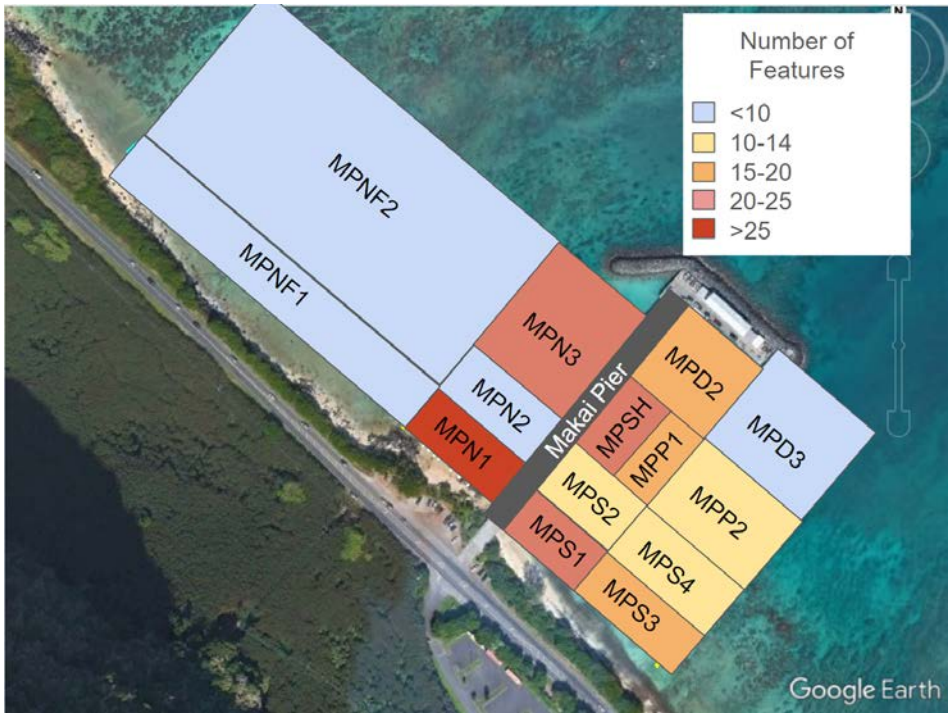

Figure S9. The ranges of total number of features observed during the semi-quantitative surveys in each zone around the pier.

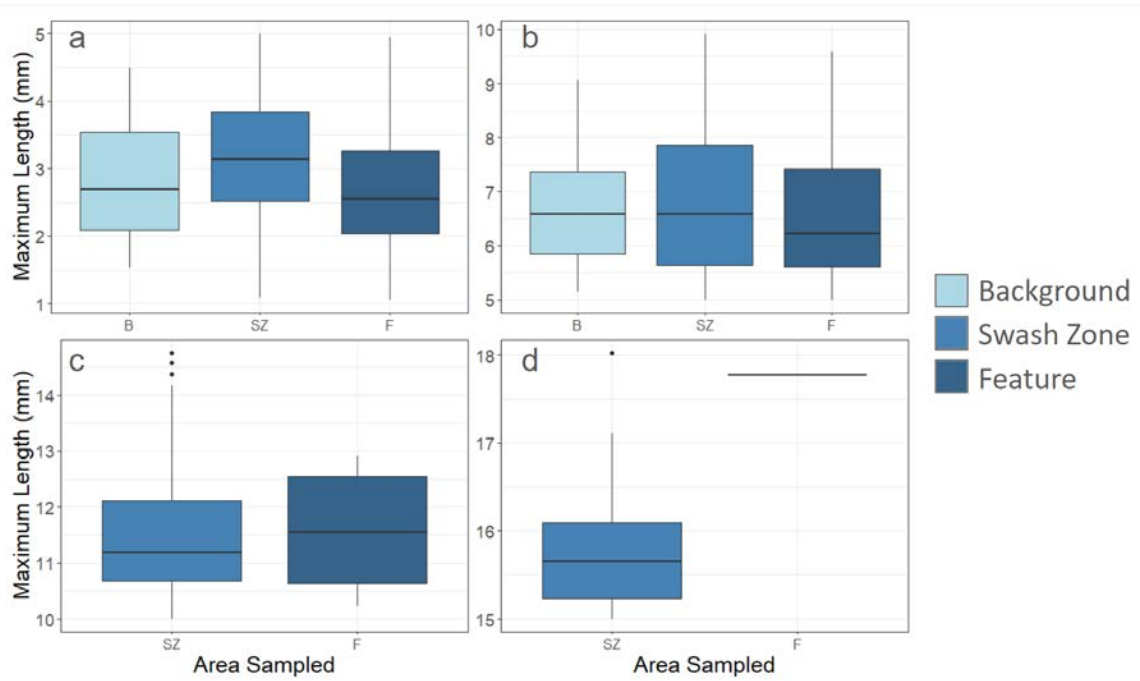

Figure S10. Distributions of microplastic maximum length (mm), excluding line, between the background (B), swash zone (SZ), and Features (F) and for sizes between a) 0-5 mm, b) 5-10 mm, c) 10-15 mm, and d) > 15 mm.